MARTIN MARIETTA ENERGY SYSTEMS LIBRARIES
3 4456 0360681 8

CENTRAL RESEARCH LIBRARY
DOCUMENT COLLECTION

ORNL-1610
Chemistry-Separation Processes
for Plutonium and Uranium

AEC RESEARCH AND DEVELOPMENT REPORT

LABORATORY DEVELOPMENT OF THE THOREX PROCESS: PROGRESS REPORT FEBRUARY 1, 1953 TO JULY 31, 1953

A. T. Gresky
M. R. Bennett
S. S. Brandt
W. T. McDuffee
B. G. Ryle
J. E. Savolainen
R. P. Wischow

Classification Cancelled
Or Changed To
By Authority Of
By Date

CENTRAL RESEARCH LIBRARY
DOCUMENT COLLECTION
LIBRARY LOAN COPY
DO NOT TRANSFER TO ANOTHER PERSON
If you wish someone else to see this document, send in name with document and the library will arrange a loan.

OAK RIDGE NATIONAL LABORATORY
OPERATED BY
CARBIDE AND CARBON CHEMICALS COMPANY
A DIVISION OF UNION CARBIDE AND CARBON CORPORATION
UCC
POST OFFICE BOX P
OAK RIDGE, TENNESSEE

RESTRICTED DATA
[redacted]

[redacted]

Report Number: ORNL-1610

This document consists of 104 pages. Number 4 of 141 copies. Series A.

Contract No. W-7405, eng 26

CHEMICAL TECHNOLOGY DIVISION

Chemical Development Section

LABORATORY DEVELOPMENT OF THE THOREX PROCESS: PROGRESS REPORT, FEBRUARY 1, 1953 TO JULY 31, 1953

A. T. Gresky, Problem Leader
M. R. Bennett
S. S. Brandt
W. T. McDuffee
B. G. Ryle
J. E. Savolainen
R. P. Wischow

Technicians:

R. C. Lovelace
J. F. Talley
C. T. Thompson

DATE ISSUED:

APR 9 1954

OAK RIDGE NATIONAL LABORATORY
Operated by
CARBIDE AND CARBON CHEMICALS COMPANY
A Division of Union Carbide and Carbon Corporation
Post Office Box P
Oak Ridge, Tennessee

[redacted]

MARTIN MARIETTA ENERGY SYSTEMS LIBRARIES

3 4456 0360681 8

ORNL 1610
Chemistry-Separation Processes
for Plutonium and Uranium

INTERNAL DISTRIBUTION

1. C. E. Center
2. Biology Library
3. Health Physics Library
4-5. Central Research Library
6. Reactor Experimental Engineering Library
7-11. Laboratory Records Department
12. Laboratory Records, ORNL R.C.
13. C. E. Larson
14. L. B. Emlet (K-25)
15. J. P. Murray (Y-12)
16. A. M. Weinberg
17. E. H. Taylor
18. E. D. Shipley
19-20. F. L. Culler
21. F. C. VonderLage
22. R. C. Briant
23. J. A. Swartout
24. C. P. Keim
25. J. H. Frye, Jr.
26. S. C. Lind
27. A. H. Snell
28. A. Hollaender
29. M. T. Kelley
30. K. Z. Morgan
31. T. A. Lincoln
32. R. S. Livingston
33. A. S. Householder
34. C. S. Harrill
35. C. E. Winters
36. D. W. Cardwell
37. E. M. King
38. W. K. Eister
39. F. R. Bruce
40. W. B. Lanham
41. H. K. Jackson
42. H. E. Goeller
43. D. D. Cowen
44. J. A. Lane
45. E. M. Shank
46. B. F. Bottenfield
47. A. C. Jealous
48. W. E. Unger
49. A. T. Gresky
50. M. R. Bennett
51. S. S. Brandt
52. W. T. McDuffee
53. B. G. Ryle
54. J. E. Savolainen
55. R. P. Wischow

EXTERNAL DISTRIBUTION

56-63. Argonne National Laboratory
64. Armed Forces Special Weapons Project (Sandia)
65. Armed Forces Special Weapons Project, Washington
66-68. Atomic Energy Commission, Washington
69-71. Brookhaven National Laboratory
72-73. California Research and Development Company
74. Carbide and Carbon Chemicals Company (C-31 Plant)
75-77. Carbide and Carbon Chemicals Company (K-25 Plant)
78-79. Carbide and Carbon Chemicals Company (Y-12 Plant)
80. Chicago Patent Group
81. Commonwealth Edison Company
82. Detroit Edison Company
83. Dow Chemical Company (Rocky Flats)
84-89. duPont Company, Augusta
90. duPont Company, Wilmington
91. Foster Wheeler Corporation

92-95. General Electric Company, Richland
96. Hanford Operations Office
97. Iowa State College
98-101. Knolls Atomic Power Laboratory
102-103. Los Alamos Scientific Laboratory
104. Massachusetts Institute of Technology (Benedict)
105. Monsanto Chemical Company
106. Mound Laboratory
107. Naval Research Laboratory
108-111. New York Operations Office
112-113. North American Aviation, Inc.
114. Patent Branch, Washington
115-118. Phillips Petroleum Company
119-122. University of California Radiation Laboratory, Berkeley
123-124. University of California Radiation Laboratory, Livermore
125-126. Vitro Corporation of America
127-141. Technical Information Service, Oak Ridge

CONTENTS

	Page No.
0.0 ABSTRACT	xi
1.0 INTRODUCTION	1
2.0 SUMMARY	2
3.0 CHANGES IN THOREX FLOWSHEET	3
3.1 Neutralization of the BU Stream	3
4.0 GENERAL PROCESS STUDIES	7
4.1 Laboratory-Scale Demonstration of Thorex Process at Full Activity Level	7
4.1.1 Feed Preparation	
4.1.2 Column Operation	9
4.1.3 Conditions of the Run	9
4.1.4 Typical Analyses of Product and Waste Streams at Steady State	
4.1.5 Column Operating Difficulties	14
4.1.6 B-Column	16
4.1.7 Protactinium Recovery	16
4.2 Feed Clarification	21
4.2.1 Effect of Acid Concentration on Coagulation of Siliceous Material	22
4.2.2 Change in Acidity of Feed During Evaporation	22
4.2.3 Countercurrent Experiments on Digested Feeds	24
4.2.4 Boiling and Freezing Points of Thorex Feed Solution During Evaporation	27
4.2.5 Evolution of Fluoride During Evaporation	27
4.2.6 Removal of Fission Products from Digested Thorex Feed Solutions by Adsorbents	27

Page No.

4.3 Ruthenium Decontamination 33

4.3.1 Isolation of Ruthenium Species 34

4.3.2 Head-End Treatment 38

4.3.3 Effects of Additives in the Scrub Section 41

4.3.4 Disproportionation Rate of the Extractable Ruthenium Species 46

4.4 Silica Gel Adsorption of Protactinium from the AP Stream 46

4.4.1 Batch Method for Scouting Experiments 49

4.4.2 Variables Affecting Adsorption 50

4.4.3 Changes in Silica Gel and DIBC Resulting from Irradiation 57

5.0 APPENDIX

5.1 Preliminary Investigation of a TBP Extraction Process for recovering U-233 from the CU Stream 59

5.2 Solvent Diluent Studies 66

5.2.1 Philosophy of Solvent Handling in the Thorex Process 66

5.2.2 Nitric Acid Degradation of Diluents Catalyzed by Mercury 68

5.3 Spectrographic Analysis of Organic Solid Contaminants 71

5.4 Tentative Chemical Flowsheet for the Decontamination and Recovery of U-235 from Irradiated Uranium-Aluminum Alloys, Using a 1.5% TBP Extraction 71

5.5 Decontamination of Thorium by Recrystallization Methods 76

5.6 Properties for Monitoring Sodium Carbonate Solution Concentrations and Consumptions 78

5.7 Composition of Diban Solutions 86

5.8 Preparation of Soluble Niobium Nitrate Solutions for Tests of Protactinium Adsorbability on Silica Gel 86

Page No.

5.9 Thorium Distribution at Equilibrium between the Aqueous and Organic Phases in the A-Column 88

TABLES

3-1 Data from Countercurrent Demonstration of Modified B-Column Operation Using Two-Strip Scheme 6

4-1 Analyses of Product and Waste Streams from the A-Column during Equilibrium Operation of Nonradioactive Start-up 11

4-2 Analyses of Product and Waste Streams from B- and C-Columns during Radioactive Thorex Run 12

4-3 Analysis of Flowing Stream Samples Taken at Steady State Operation 13

4-4 Effect of Reduced AX Flow Rate on Decontamination of Thorium in the BT Stream 15

4-5 Physical and Chemical Data for the A-Column Interfacial Solids from Unfiltered Irradiated Thorium Slug Solution Feeds 19

4-6 Corrosion of Stainless Steels During High Temperature Reflux in Digestion Procedure (100-hr Tests) 26

4-7 Approximate Boiling and Freezing Points of Thorex Feed Solution During Digestion under Proposed Process Conditions 28

4-8 Data from Typical Evaporation of Thorex Dissolver Solution, When an Essentially Stoichiometric Amount of Nitric Acid Is Used in Dissolution 29

4-9 Data from Typical Evaporation of Dissolver Solution, When a Twofold Excess of Nitric Acid Is Used in Dissolution 30

4-10 Observed Evolution of Fluoride During Evaporation of Thorex Dissolver Solution 31

4-11 Effectiveness of Adsorbents for Activity Removal from Thorex Digested Feeds 32

4-12 Adsorption of Activity on Filtrol Following Digestion in Presence of Type 309SCb Stainless Steel 33

4-13 Distribution of Ruthenium Species in Aqueous and Organic Phases of Extraction (16-stage) Apparatus 36

Page No.

4-14 Effect of Head-End Treatments on Decontamination: Summary of Fission Product Decontamination Factors 39

4-15 Summary of A-Column D.C.'s (O/A) for Ruthenium and Gross Beta at the Feed Plate, Extraction Section, and Scrub Section following Various Head-End Treatments 40

4-16 Fission Product Distribution in A-Column: Typical Countercurrent Data When Using the AF Digestion Procedure 43

4-17 Effect of AS Additives on Distribution Coefficient of Extractable Ruthenium 45

4-18 Analytical Data Showing the Contribution of Thorium Metal, Aluminum Jacket, and Corrosion to the Presence of Fe, Nb, Cr, Ni, and Zr in Thorex AF Solutions 48

4-19 Comparison of Results Obtained in Column Runs and Batch Runs 49

4-20 Effect of Various Materials on Silica Gel Adsorption of Pa^{233} from Thorex AP Solutions Containing Ferric Ion 54

5-1 Components of Synthetic CU Stream 60

5-2 Change in Phosphate Concentration During Evaporation 60

5-3 Data from Batch Countercurrent Extraction of Uranium 65

5-4 Results of Contacting Amsco 125-82 with 10 M HNO_3 Containing Increasing Amounts of Mercury 69

5-5 Summary of Conditions Observed in the A and B Columns of the 25 Process Flowsheet 74

5-6 Decontamination of Mantle Grade Thorium Nitrate by Recrystallization 79

5-7 The pH and Conductivities of Sodium Carbonate Solutions at 25°C 80

5-8 Conductivity and pH of 0.1 M Na_2CO_3 Titrated with HNO_3 81

5-9 Conductivity and pH of 0.2 M Na_2CO_3 Titrated with HNO_3 82

5-10 Results of Chemical Analyses of Diban Samples 87

5-11 Thorium Distribution between Aqueous and Organic Phases in the A-Column Extraction Section 89

[redacted]

Page No.

5-12 Thorium Distribution between Aqueous and Organic Phases in the A-Column Extraction Section 90

5-13 Distribution of Thorium between Aqueous and Organic Phases in the A-Column Scrub Section 91

FIGURES

3-1 Thorex Process Chemical Flowsheet - July 1953 5

4-1 Scintillation Spectrogram of A-Column Interfacial Solids (Run H) 17

4-2 Scintillation Spectrogram, A-Column Feed (Run H) 18

4-3 Nitric Acid Concentration vs. Thorium and Aluminum Concentrations, Observed During Evaporation of Thorex Dissolver Solutions of Various Initial Acidities 23

4-4 Corrosion Rate of Unwelded Stainless Steels as Functions of Stages of Evaporation of a Solution 1.0 M in Thorium, 0.4 M in Aluminum, and 6.5 M in Nitric Acid 25

4-5 Separation of Ruthenium Species: Ruthenium D.C.(O/A) vs. Stage Number in Batch Countercurrent Extraction Apparatus 35

4-6 Ruthenium D.C. (O/A) in the AU Stream as a Function of Sodium Hydrosulfite Concentration in the AS Stream 42

4-7 Disproportionation of the Extractable Ruthenium Species: Ru β Distribution Coefficient as a Function of the Holdup Time in the AU Stream 47

4-8 Effect of Niobium on Adsorption of Protactinium on Silica Gel from Synthetic Thorex AP Streams 51

4-9 Effect of Iron and Chromium on Adsorption of Protactinium on Silica Gel from Synthetic Thorex AP Stream 52

4-10 Effect of $CrO_4^{=}$ in Presence of 0.003 M Fe^{3+} (0.118 N acid-deficient aluminum nitrate nonahydrate) on Adsorption and Carrying of Protactinium from Synthetic Thorex AP Solution 53

		Page No.
4-11	Effects of Tracer History: Room Temperature Digestion of Nonadsorbable Pa^{233} Tracer in 7 N HNO_3	56
5-1	Percentage Removed of the Total TBP Initially Present as a Function of the Boildown Ratio	61
5-2	Uranium Concentration in Residue as a Function of the Boildown Ratio	63
5-3	Nitric Acid and TBP Concentrations in Residue as a Function of the Boildown Ratio	64
5-4	Tentative Flowsheet for Recovery and Decontamination of U^{235} from Irradiated Uranium-Aluminum Alloys	73
5-5	Tentative Method for Purifying Mantle Grade $Th(NO_3)_4$ by Recrystallization	77
5-6	Conductivity of Aqueous Na_2CO_3 Solution as a Function of Concentration at 25°C	83
5-7	Conductivity and pH of 0.1 M Na_2CO_3 Titrated with 10.1 M HNO_3	84
5-8	Conductivity and pH of 0.2 M Na_2CO_3 Titrated with HNO_3	85

PREVIOUS REPORTS ISSUED IN THIS SERIES

ORNL-1367, "Progress Report: Laboratory Development of the Thorex Process," by A. T. Gresky, M. R. Bennett, S. S. Brandt, W. T. McDuffee, and J. E. Savolainen (Dec. 17, 1952).

ORNL-1431, "Laboratory Development of the Thorex Process: Progress Report, September 30, 1952," by A. T. Gresky, M. R. Bennett, S. S. Brandt, K. L. Mattern, W. T. McDuffee, J. E. Savolainen, and R. P. Wischow (Mar. 16, 1953).

ORNL-1518, "Laboratory Development of the Thorex Process: Progress Report October 1, 1952 to January 31, 1953," by A. T. Gresky, M. R. Bennett, S. S. Brandt, W. T. McDuffee, B. G. Ryle, J. E. Savolainen, and R. P. Wischow (July 14, 1953).

[redacted]

0.0 ABSTRACT

Laboratory-scale studies on the Thorex process, February 1 - July 31, 1953, have led to the recommendation that excess acid be removed from the organic stream in a slightly longer B-column with very dilute nitric acid rather than in a separate column with "acid-deficient" aluminum nitrate as formerly. A head-end evaporation-reflux treatment of the feed is recommended to prevent loss of thorium, to coagulate colloidal siliceous material and thus minimize emulsions in later steps, and to decrease the ruthenium in the product stream. Pa^{233} adsorption by silica gel was inhibited by niobium, ferric, or chromic ions.

[redacted]

1.0 INTRODUCTION

Laboratory-scale studies during the period February 1 - July 31, 1953 are reported here, including the results of a full-activity-level demonstration of the Thorex process in 0.5-in.-diameter pulse columns. Cost studies made on the continuous dissolution procedure indicated that in small plants (< 3 metric tons/day) there is no economic advantage in continuous as compared with batch dissolution, and a batch dissolution process is incorporated in the July 1953 flowsheet.

The results of the run on highly radioactive material indicated the need for head-end treatment of the metal solution, and a feed preparation tank will be installed in the Thorex pilot plant where this may be carried out.

A satisfactory method of recovering Pa^{233} has not yet been developed, and design of a protactinium recovery unit is awaiting further laboratory study on this problem.

2.0 SUMMARY

Recommended process changes reflected in the July 1953 flowsheet include lengthening of the B-column to accommodate a split stream, one part being 0.24 N HNO_3 to strip the thorium and the other part 0.005 N HNO_3 to scrub excess acid from the organic stream before it enters the C-column and thus increase the U^{233} stripping in the C-column. The neutralization column in which this was formerly accomplished with "acid-deficient" aluminum nitrate solution has been discarded.

An evaporation-reflux treatment of the feed before it enters the extraction (A) column was shown to dissolve the thorium precipitate, and thus prevent loss of thorium, and coagulate the siliceous precipitate that forms in the dissolver when highly radioactive metal is processed. The coagulated material is filtered off. Emulsion formation in the columns is minimized by the removal of the siliceous material. This treatment was also shown to convert some of the ruthenium present to a nonextractable form and thus increase the ruthenium decontamination of the product.

Studies on Pa^{233} isolation showed that protactinium adsorption by silica gel is inhibited by niobium, iron, chromium, calcium, or magnesium ions or hydrogen peroxide. Phosphate or sulfate ions decreased the interference of niobium, and excess chromate ion decreased the interference of ferric and chromic ions. Beryllium did not affect protactinium adsorption.

3.0 CHANGES IN THOREX FLOWSHEET

The principal changes in the Thorex process, as reflected in the July 1953 flowsheet (see Fig. 3-1), were concerned with (1) the choice of a batch dissolving procedure as being more economical* and (2) the elimination of the neutralization column and the substitution for the neutralization step of a very dilute nitric acid scrub in the top of the B-column.

3.1 Neutralization of the BU Stream
(W. T. McDuffee, A. T. Gresky)

The scheme for BU neutralization suggested in ORNL-1518 (i.e., scrubbing with the adjusted AS stream) was reviewed and found to be uneconomical and somewhat difficult in practical operation. A simpler method has been devised which involves scrubbing the BU stream with very dilute nitric acid, the BX stream, in the upper section of the B-column, just before it leaves to enter the C-column (see Fig. 3-1). Pure water cannot be used because with it emulsions are formed.

About eleven stripping stages in the B-column, three more than previously used, were required to strip the thorium and reduce the BU acidity from 0.04 to less than 0.01 N HNO_3 (see Table 3-1), the concentration required in the C-column for efficient U^{233} stripping. The number of stages and/or the column height required to accomplish this can be shown to depend on the relative flow ratios and the acidities of the proposed BX and B'X streams; for example, conditions which may be varied to control the height of the BX stripping section are:

BX		+ B'X		→ B'X + BX	
Flow Ratio	HNO_3 (N)	Flow Ratio	HNO_3 (N)	Flow Ratio	HNO_3 (N)
1.0	0.005[a]	4.8	0.24	5.8	0.2
2.0	0.005	3.8	0.30	5.8	0.2
3.0	0.005	2.8	0.41	5.8	0.2

(a) Required to ensure absence of emulsification during phase mixing.

*D. L. Foster and A. R. Irvine, "Economic Evaluation of Continuous Dissolving," ORNL CF-53-3-154 (March 16, 1953).

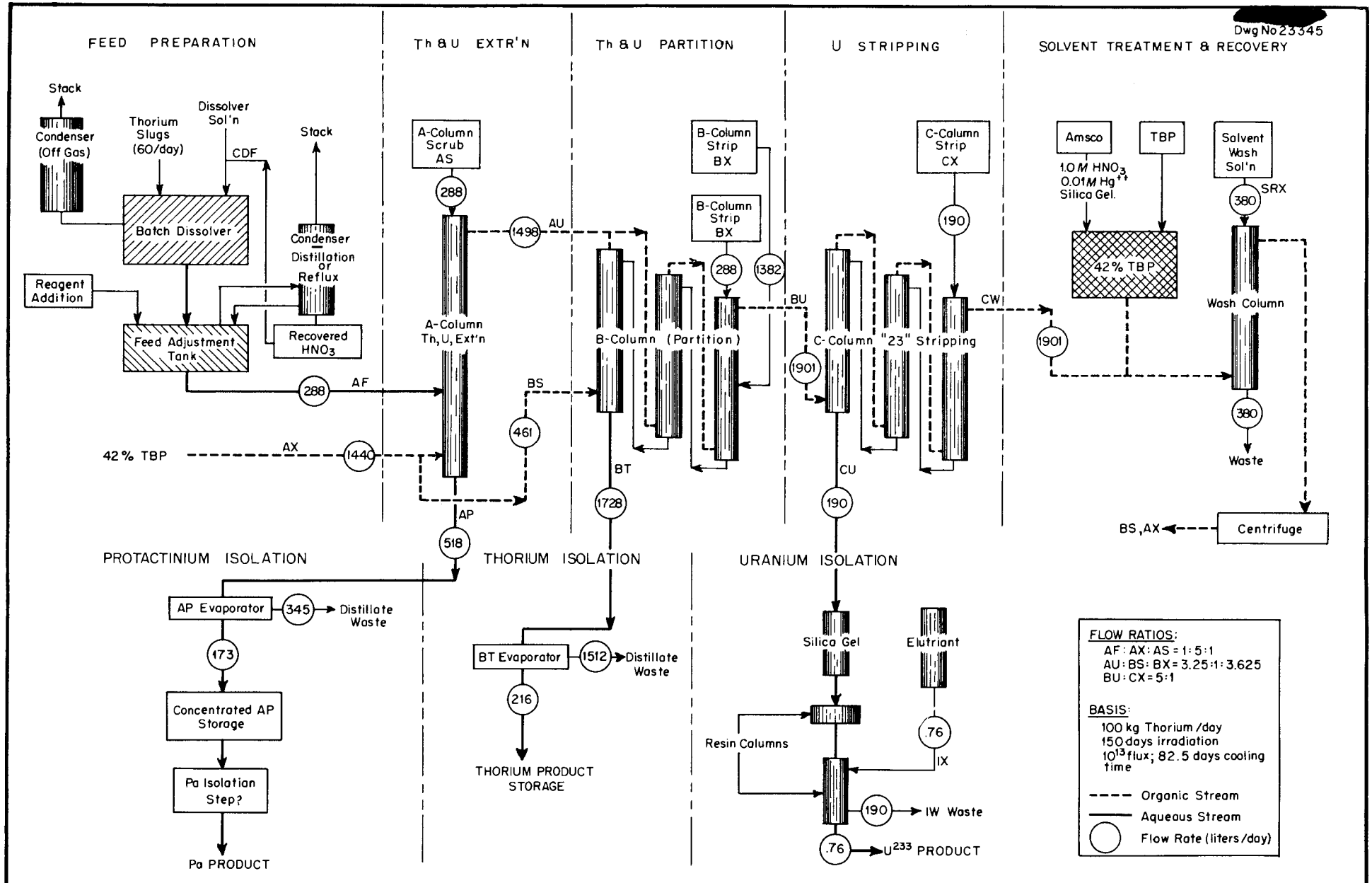

SECRET

Fig. 3-1. THOREX PROCESS CHEMICAL FLOWSHEET – July 1953

APPROXIMATE STREAM COMPOSITIONS

CDF	~13 N HNO_3, ~0.1 N F^-, ~0.004 M Hg^{2+}
AF	1.5 M Th, 0.6 M Al, 0.5 M HNO_3, 0.3 g U per liter
AS	0.6 M Al, 0.75 M HNO_3-deficient, 0.002 M $PO_4^{\equiv}$
AX	42.5% TBP, 57.5% preconditioned Amsco 125-82, 0.0 M HNO_3
AU	42.5% TBP, 0.29 M Th, 0.06 g of U per liter, 0.0 M HNO_3
BS	(Same as AX)
B'X	0.24 N HNO_3
BX	0.005 N HNO_3
BU	42.5% TBP, 0.045 g of U per liter, ~0.002 N HNO_3
BT	0.25 M Th, 0.15 M HNO_3
Thorium Product	2.0 M Th, 1.2 M HNO_3
AP	0.67 M Al, 0.15 M HNO_3-deficient
CX	0.005 to 0.01 M HNO_3
CU	0.5 g U per liter, 0.01 to 0.05 N HNO_3
CW	42.5% TBP, $\angle$0.001 M HNO_3
IX	2.0 M ammonium acetate, 0.4 M acetic acid, pH 5.85
SRX	0.1 M Na_2CO

Table 3-1

Data from Countercurrent Demonstration of Modified B-Column Operation Using Two-Strip Scheme

Feed, synthetic AU: 43% TBP in Amsco 125-90W; Th, 70 mg/ml; U, 0.094 mg/ml; HNO_3, 0.0 N

Scrub, BS: 43% TBP in Amsco 125-90W; diluent pretreated with 10 M HNO_3, $Ca(OH)_2$, and silica gel; the 43% mixture treated with $Ca(OH)_2$

Strip 1, BX: 0.012 N HNO_3

Strip 2, B'X: 0.23 N HNO_3

Flow ratios, Feed/1-St/2-St/Sc: AU/BX/B'X/BS = 5.2/1.0/4.8/1.6

6 scrub stages; 8 strip-2 stages; 3 strip-1 stage

Stage No.	Organic			Aqueous		
	Thorium (mg/ml)	Uranium (mg/ml)	H^+ (N)	Thorium (mg/ml)	Uranium (mg/ml)	H^+ (N)
11 St	0.005[a]	0.048	0.01	---	---	---
10 St	0.005[a]	0.07	0.025	0.024	0.065	0.175
8 St	0.014[a]	0.052	0.044	0.015	0.035	0.23
6 St	0.08	0.089	0.047	0.412	0.047	0.245
4 St	3.0	0.08	0.073	11.8	0.016	0.205
2 St	23.8	0.054	0.091	39.2	0.006	0.260
1 Sc	50.0	0.045	0.072	72.0	0.0043	0.198
3 Sc	51.0	0.015	--	72.0	0.00073	0.195
5 Sc	48.5	0.002	--	69.4	0.00012	0.195
6 Sc	--	--	--	59.0	0.00004	0.180

(a) Analyses subject to question in thorium concentration range of 5 to 20 μg/ml.

Adjustments can be made so that the aqueous acidities in stages 8 and 7 are maintained at about 0.2 N HNO_3, i.e., equivalent to the salting strength required for uranium extractability and/or prevention of undue uranium reflux and retention in the B-column. (Note: These points are considered necessary to forestall possible losses of U^{233} by uncontrolled buildup of uranium concentration, by reflux, throughout the B-column in conjunction with possible fluctuations of flow-rate controls and/or AU thorium concentrations, which govern the uranium distribution in the B-column.)

It can be seen that adjustments of the composition and flow ratios of the two streams permit direct control of the BU acidity and indirect control of acidity and/or uranium concentration in the CU stream, i.e., according to the desired flow ratio, or flow rate, of the CX stream.

4.0 GENERAL PROCESS STUDIES

4.1 Laboratory-Scale Demonstration of Thorex Process at Full Activity Level

(W. T. McDuffee, A. T. Gresky, C. V. Ellison, S. S. Brandt, R. P. Wischow)

In order to show how the Thorex process would operate when full-activity-level feed was used, a run was made in 0.5-in.-diameter pulse columns on an irradiated thorium slug (approximately 1000 g of U^{233} per ton) which had cooled for about 180 days. The results of the run indicated that thorium and uranium losses of less than 0.1% and of less than 0.01%, respectively, might be expected in the solvent-extraction steps. Losses due to undissolved thorium ("blue thorium") were not determined, but were estimated to be of the order of 1.0%. Decontamination of the thorium and uranium products was not satisfactory, primarily because of some extremely radioactive interfacial solid material carried over from the top of the extraction column to the strip columns. This indicated the need for

clarification of the dissolver solution before it is fed to the A-column.

An attempt was made to recover protactinium from the total AP stream following concentration and acidification by a batch extraction using diisobutyl carbinol. Less than 1.0% was extracted. A thorough analysis of causes for this failure was not possible; however, it was found that 10 to 20% of the total Pa^{233} had plated out on the walls of the stainless steel evaporator used for concentrating the AP stream.

Owing to time limitations imposed by other processing programs, the B- and C-column geometries were not optimized, and demonstrations of satisfactory uranium-thorium separation in the B-column and U^{233} recovery in the C-column were not possible. The principal benefit from the run was the information obtained on (1) effects of radiation on the nature of insoluble feed constituents and attendant effects on product losses and decontamination and (2) the unfavorable effects of AP evaporation on protactinium recovery.

4.1.1 Feed Preparation

A 6-in. aluminum-jacketed thorium slug that had been irradiated (approximately 1000 g of U^{233} per ton) at Hanford and cooled for about 180 days was used. It was dissolved in 3.6 liters of 70% HNO_3, in a stainless steel dissolver, at 110 to 115°C using as catalysts 0.005 M Hg^{2+} and 0.075 M F^-. The dissolver solution was adjusted to flowsheet feed conditions by dilution with water and nitric acid. The aluminum concentration of the adjusted feed was slightly higher than flowsheet conditions because a sliver* of thorium that did not dissolve was removed

---

* Subsequent dissolution of this thorium sliver in a glass dissolver revealed the presence of a blue insoluble material that had a spectrographic analysis as follows: thorium, very strong; silicon and aluminum, moderate; calcium, sodium, lead, and copper, weak; magnesium, boron, iron, and cobalt, trace. This highly insoluble material represents a potential loss of thorium and/or U^{233} of 0.6 to 1.5%; however, a method for dissolving it has been recently developed. This material apparently forms during the irradiation, since it has not been observed in nonradioactive metal dissolver solutions.

in order to avoid the long time required for complete dissolution.

While still in the dissolver, the adjusted feed was cooled to room temperature, made 0.005 M in HIO_4, and allowed to digest for 15 min; it was then made 0.5 M in formic acid and the temperature was raised to 108 to 110°C for 3 hr. After cooling, the feed was transferred, without filtering, to a stainless steel holding tank.

4.1.2 Column Operation

All the columns were of glass, 0.5 in. i.d., with stainless steel fittings, plates, and spacers. Plate spacing in the columns was 1.0 in., except in the A-column extraction section which was 0.5 in.

The organic stream was cascaded from A-column to B-column to C-column. All aqueous streams were fed by pumps and could be closely controlled. The flows of primary solvent streams were controlled by throttling a pressurized stream from a head tank, but close control by this method was not possible, and flow rates of organic streams were not constant.

The A-column was equipped with an entrainment separator in the AU line. There was about 1 hr holdup in the AU line between the A- and B-columns, including that in the entrainment separator. There was about 15 min holdup in the BU transfer line.

4.1.3 Conditions of the Run

The compositions and flow ratios of the entering streams were:

AF	Th, 1.5 M HNO_3, 0.5 N Al, 0.8 M U^{233}, 0.36 mg/ml Gross β, 4.6×10^9 c/m/ml Pa β, 3.71×10^9 c/m/ml Ru β, 6.3×10^6 c/m/ml Nb β, 1.15×10^7 c/m/ml Zr β, 4.9×10^7 c/m/ml TRE β, 2.58×10^8 c/m/ml	Flow rate, 90 ml/hr Flow ratio = 1.0

AS	Al, 0.6 M HNO_3, 0.75 N acid deficient	Flow ratio = 1.0
AX	TBP, 42.5% Amsco 125-90W (preconditioned), 57.5% (diluent mixture also preconditioned by 1 hr contact with 60 g of $Ca(OH)_2$ per liter and filtering)	Flow ratio = 5.0
B'X	HNO_3, 0.24 N	Flow ratio = 4.8
BX	HNO_3, 0.01 N	Flow ratio = 1.0
BS	TBP, 42.5% Amsco 125-90W, 57.5% (preconditioned)	Flow ratio = 1.6
CX	HNO_3, 0.01 N	Flow ratio = 1.32

The column heights were:

A-column	4 ft of extraction, 6 ft of scrub
B-column	2 ft of scrub, 4 ft of 0.24 N HNO_3 strip, 2.0 ft of 0.01 N strip
C-column	5 ft of strip

4.1.4 Typical Analyses of Product and Waste Streams at Steady State

A-column. A-column losses were low (see Table 4-1). No samples of the AU and AP streams were taken after the active feed was introduced to the columns, but samples taken during the nonradioactive start-up of the run were analyzed. The values obtained were used to calculate losses.

B- and C-columns. Table 4-2 gives analyses of the streams from the B- and C-columns and the decontamination factors obtained. The somewhat high losses and poor separation factors were the result of nonoptimum column geometries.

Detailed Analyses. Detailed analyses of flowing stream samples are given in Table 4-3.

Table 4-1

Analyses of Product and Waste Streams from the A-column during Equilibrium Operation of Nonradioactive Start-up

Stream	Composition
AU (uranium product)	Th, 67.4 mg/ml U, 0.19 mg/ml H^+, 0.004 N acid deficient
AP (protactinium product)	Th, 0.095 mg/ml (0.049% of Th in AU) U, 0.000037 mg/ml (0.007% of U in AU[a]) H^+, 0.04 N acid deficient

(a) This figure based on uranium concentration of 1.0 mg/ml in feed in nonradioactive runs.

Table 4-2

Analyses of Product and Waste Streams from B- and C-Columns during Radioactive Thorex Run

Stream	Composition		Product Decontamination Factor
BT (thorium product)	Th	57 mg/ml (~98.2% recovery)	
	H^+	0.15 N	
	U^{233} α	1.2×10^4 c/m/ml (~1.5% loss)	
	Gross β	9×10^4 c/m/ml	8.5×10^3
	Pa β	2×10^4 c/m/ml	3×10^4
	Ru β	1×10^4 c/m/ml	100
	Nb β	2×10^3 c/m/ml	9.5×10^2
	Zr β	2×10^3 c/m/ml	4.0×10^3
	TRE β	2×10^3 c/m/ml	2.2×10^4
CU (uranium product)	U^{233} α	2.9×10^6 (~96% recovery)	
	H^+	0.1 N	
	Th	0.2 mg/ml (U-Th sepn. factor ~10^4	
	Gross β	6.0×10^3 c/m/ml	5.9×10^5
	Ru β	4.0×10^3 c/m/ml	1.2×10^3
	Nb β	700 c/m/ml	1.3×10^4
	Zr β	50 c/m/ml	7.7×10^5
	TRE β	20 c/m/ml	1×10^7
CW (waste organic)	Th	0.01 mg/ml	
	H^+	---	
	U^{233} α	1×10^3 c/m/ml (~0.25% loss)	
	Gross β	9×10^3 c/m/ml	
	Ru β	4×10^3 c/m/ml	
	Nb β	200 c/m/ml	
	Zr β	300 c/m/ml	
	TRE β	20 c/m/ml	

Table 4-3

Analysis of Flowing Stream Samples Taken at Steady State Operation

AF analysis:
Th: 350 mg/ml
Al: 0.8 M
HNO_3: 0.5 N

U^{233}: 0.36 mg/ml
Gross β: 4.6×10^9 c/m/ml
Pa β: 3.7×10^9 c/m/ml

TRE β: 2.6×10^8 c/m/ml
Zr β: 4.9×10^7 c/m/ml
Nb β: 1.2×10^7 c/m/ml

Ru β: 6.3×10^6 c/m/ml

Operation Time (hr)	Th (mg/ml)	H^+ (N)	Activities (c/m/ml)						
			Gross β	Pa β	Ru β	Nb β	Zr β	TRE β	U^{233} α
BT Stream									
26	54.6	0.09	1.18×10^5	1.36×10^5	6.9×10^3	4×10^3	4.4×10^3	1×10^3	---
31	49.6	0.07	9.25×10^4	1.47×10^4	---	---	---	---	2.78×10^4
32	54.4	---	1.08×10^5	4.49×10^4	1.75×10^4	4.73×10^3	1.44×10^3	1.86×10^4	1.2×10^4
33	53.4	0.14	6.97×10^4	1.64×10^4	---	---	---	---	1.65×10^4
34	54.0	---	7.08×10^4	1.6×10^4	1.4×10^4	7×10^2	7×10^2	2.5×10^3	2.97×10^4
36	50	0.18	7.87×10^4	2.1×10^4	1.35×10^4	1.7×10^3	1.83×10^3	6.0×10^3	4.94×10^4
38	50	0.16	6.2×10^4	1.17×10^4	1.0×10^4	3.5×10^2	1×10^3	4.6×10^3	3.74×10^4
CU Stream									
27	0.24	0.07	7.61×10^3	---	6.27×10^3	718	70	15	3.76×10^6
29	0.13	0.07	5.97×10^3	---	2.9×10^3	740	44	23	2.3×10^6
31	0.20	0.07	8.85×10^3	---	6.0×10^3	300	10	20	1.89×10^6
33	0.13	0.07	1.28×10^4	---	1.0×10^4	150	80	0	2.1×10^6
35	0.17	0.07	1.23×10^4	---	9.86×10^3	200	20	10	1.82×10^6
37	0.18	0.07	1.24×10^4	---	1.0×10^4	650	35	10	1.61×10^6
CW Stream									
28	0.013	---	1.07×10^4	---	2.64×10^3	116	512	30	1.45×10^3
30	0.021	---	1.35×10^4	---	2.6×10^3	992	968	---	2.35×10^3
32	0.014	---	8.95×10^3	---	4.89×10^3	220	290	30	4.27×10^3
34	0.005	---	4.18×10^4	---	2.5×10^3	7×10^3	2.9×10^3	30	8.75×10^3
36	0.005	---	7.35×10^3	---	4.49×10^3	180	420	15	1.43×10^3

4.1.5 Column Operating Difficulties

Flow Rate Control. Control of all aqueous streams was satisfactory throughout the run. However, the control of the organic AX and BS streams was poor, and the erratic flow rates obtained upset the column equilibrium and resulted in poor decontamination in the A-column and/or poor separation of uranium and thorium in the B-column (see Table 4.4). The most frequent happening was for the AX flow rate to drift to lower rates, causing the A-column to flood, probably because of the formation of a second organic phase of very poor settling characteristics.

The greater loading of the solvent with thorium increased both the viscosity and the density of the AU stream. Under these conditions solids are more likely to be entrained in the organic phase as a result of the reduced organic flow rate, and this may account for the lower decontamination observed. It was noted at times during the run that solid particles were occasionally suspended in the continuous organic phase in the entrainment separator that followed the A-column. It is probable that the pulse pushed these into the AU transfer line to the B-column, and that this accounted for the erratic results obtained in the BT stream. High fission product activity was later found to be associated with the solids. It is imperative that such entrained solids be eliminated from the AU stream in order to obtain the highest protactinium and fission product decontamination factors.

Effect of Plate Spacing on Extraction in the A-Column. Contact between the two phases in the extraction section was poor when 1.0-in. spacing was used, the condition of most effective contact in the scrub section. Thorium losses were excessive, 1 to 2%, under these conditions. The substitution of 0.5-in. spacing in the extraction section reduced the losses to less than 0.1%. No difficulty was encountered in the B- and C-columns in this respect.

Interfacial Solids Found in the A-Column Scrub Section. A layer of solids accumulated at the A-column interface in the radioactive run; this

Table 4-4

Effect of Reduced AX Flow Rate on Decontamination of Thorium in the BT Stream

	AX flow ratio	Th in BT	U^{233} in BT
Normal	5.2	57 mg/ml	1.5×10^4 c/m/ml
Reduced	3.5	87.6 mg/ml[a]	4×10^4 c/m/ml

Activity	Normal Flow Rate		Reduced Flow Rate	
	BT Activity Level (c/m/ml)	Decontamination Factor	BT Activity Level (c/m/ml)	Decontamination Factor
Gross β	9×10^4	8.5×10^3	9.1×10^5	1.3×10^3
Pa β	2×10^4	3.1×10^4	8.1×10^5	1.2×10^3
Ru β	1×10^4	1.0×10^2	1.3×10^4	1.3×10^2
Nb β	2×10^3	9.5×10^2	1.4×10^4	2.1×10^2
Zr β	2×10^3	4.0×10^3	1.5×10^4	8.2×10^2
TRE β	2×10^3	2.2×10^4	2.1×10^4	3.1×10^3

(a) The solvent is saturated with thorium at this concentration, and a slight increase in thorium concentration would cause two organic phases to form. This value in the BT stream would presuppose approximately 100 mg of thorium per milliliter in the AU stream at normal flow rates.

emphasized the need for an efficient entrainment separator in the AU line. A suspension of 10 to 20 mg of this solid material was withdrawn from the A-column and filtered on a fine-porosity glass filter and freed of soluble matter by washing with water and acetone. No difficulty was encountered in the filtering. As an indication of the activity retained by the solids, a radiation reading of a few milligrams of the dried powder was greater than 75 r at 2 in.

Pertinent data regarding the solid are summarized in Table 4-5. The scintillation spectrogram of the solid material (Fig. 4-1) was quite similar to that of the feed (Fig. 4-2).

4.1.6 B-Column

The revised B-column flowsheet (i.e., the flowsheet that uses a split stripping solution), which was used for the first time in this run, appeared to be feasible and not difficult in operation. The length of the strip sections and flow rates were not at an optimum, so that the U^{233}-thorium separation factors were not so high as required in process specifications. (However, the Unit Operations Section has demonstrated the feasibility of and established geometries for 2-in.-diam. column operation.)

4.1.7 Protactinium Recovery

The AP stream was continuously evaporated to about one-third its original volume during the course of the run. The evaporator was a 5 liters capacity stainless steel vessel fitted with a heating and cooling jacket, appropriate liquid level and temperature indicators, and a stirrer. At the conclusion of the run the AP concentrate was made approximately 0.75 N in HNO_3, contacted with 0.1 volume of diisobutylcarbinol for 0.5 hr, and allowed to settle for 0.5 hr. The aqueous phase was discarded, and the DIBC layer was withdrawn to suitable auxiliary equipment for protactinium recovery. However, the DIBC contained essentially no protactinium. (The Analytical Chemistry Division has experienced inextractability of protactinium in DIBC and diisopropylcarbinol as a function of niobium interference.) This

[redacted]

Dwg No19733

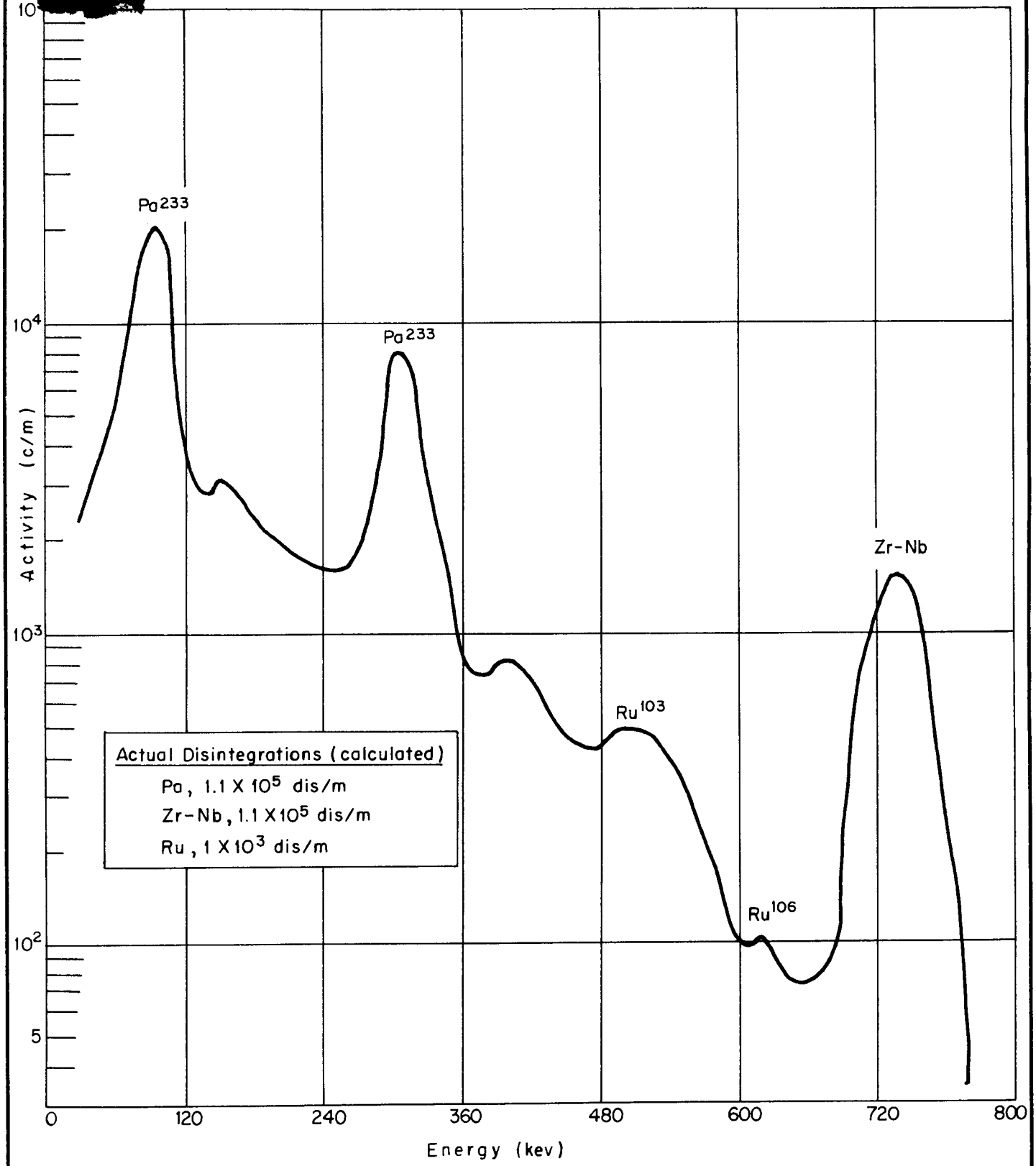

Fig. 4-1. Scintillation Spectrogram of A-Column Interfacial Solids (Run H)

[redacted]

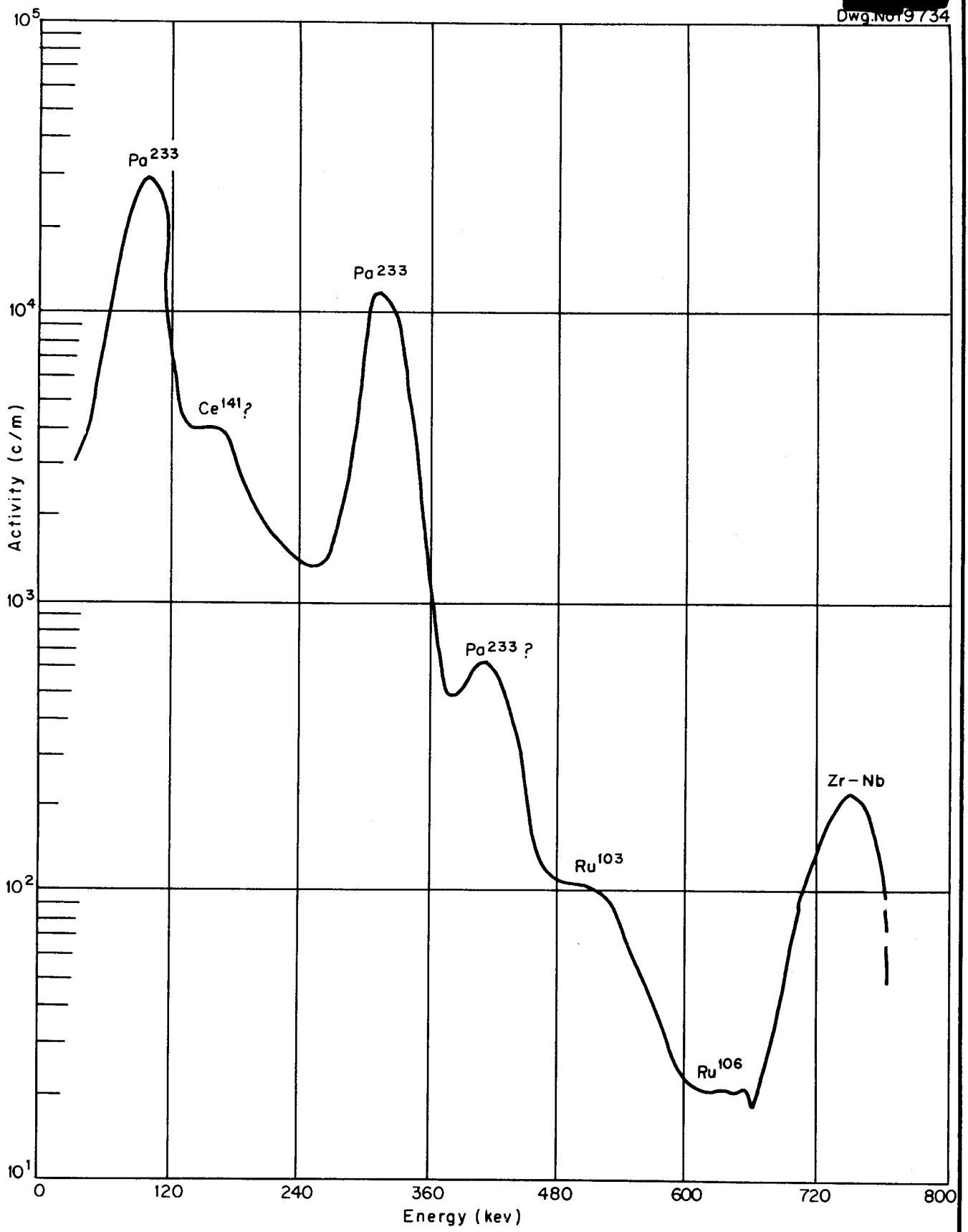

Fig. 4-2 Scintillation Spectrogram, A-Column Feed (Run H)

Table 4-5

Physical and Chemical Data for the A-Column Interfacial Solids from Unfiltered Irradiated Thorium Slug Solution Feeds

Physical properties	Color: brown to gray Texture: fine particles, which filtered readily on fine-porosity filter Density: >2.0 g/ml
Qualitative solubility tests (successive steps)	1. Almost completely insoluble in concentrated HNO_3, HCl, gluconic acid, and versene; very little activity removed from filter by 5 ml of reagent 2. Partly soluble in boiling 95% H_2SO_4; less than 5% of activity removed from filter by 5 ml of reagent 3. Completely soluble in 3% HF—20% HNO_3; more than 95% of activity removed from filter by 100 ml of reagent
Radiochemical β spectra of dissolved portion	1. HCl soluble (activities in c/m/ml) Gross β 2×10^7 Pa β 4.9×10^6 Ru β 5.3×10^5 Nb β 3.4×10^5 (a) Zr β 2.5×10^5 TRE β 1000 2. H_2SO_4 soluble (activities in c/m/ml) Gross β 3.9×10^7 Pa β 1.9×10^7 Ru β 8.2×10^5 Nb β 6.4×10^5 (a) Zr β 2.5×10^5 TRE β 750 3. HNO_3-HF soluble (activities in c/m/ml) Gross β 1.8×10^7 Pa β 2.7×10^6

Table 4-5 (Cont.)

	Ru β Nb β TRE β — 3.7×10^5 (a) 100
Suspected sources of solid material	Al: 25 to 500 ppm in Ames metal Si: 37 to 50 ppm in Ames metal Ca: 20 to 100 ppm in Ames metal Fe: 0 to 380 ppm in Ames metal Fe, Cr, Ni: corrosion products of stainless steel dissolver
Gamma spectrum (scintillation spectrometer)	Pa^{233} Nb-Zr(b) ~50% of total gamma $Ru^{103, 106}$ ~50% of total gamma Ce^{141} < 1% of total gamma Pa/Zr Masked; low if present > 10 times lower than in feed
Spectrographic analysis	Al, Si: strong(c) Ca, Fe: moderate Cr, Mn, Ni: weak Cu: very weak Mg, Sn, Th, Ti, Zr(b): trace Pd: faint trace Be, Ce, Ge, La, Li, Mo, Pt, Re, Rh, Ru, Sb, Ta, U, V, Y, Yb, Zn: sought but not found

(a) Not indicative of actual disintegrations, owing to G.M. counting efficiency. See gamma spectrum in this table and Fig. 4-1.

(b) FMPC plans to use zirconia instead of beryllia crucibles to reduce health hazard.

(c) The high insolubility of the solids suggests that refractory clays, e.g., $Al_2Si_2O_7$, $Ca_6Al_2Si_6O_{21}$, or $CaZrSi_3O_9$, may form during metallurgical processing of the thorium metal to form slugs.

experience indicated the need for further development of the extraction method. About 30% of the protactinium present plated out of the solution on the walls of the evaporator during the evaporation as indicated by subsequent decontamination steps.

4.2 Feed Clarification
(R. P. Wischow)

An evaporation-reflux procedure was developed which coagulated colloidal siliceous material and dissolved the "blue thorium" residue (see Sect. 4.1.1, p. 8, footnote). As carried out on a laboratory scale, the process consisted in evaporating water from the dissolver solution at atmospheric pressure, adding concentrated nitric acid, and refluxing the concentrated acid solution for 3 to 4 hr. The acid was then evaporated off, and the concentrated residue was adjusted to the acid, thorium, and aluminum concentrations desired for feed to the solvent extraction columns.

This coagulated siliceous material can be filtered off readily, but filtration is not mandatory since the emulsion-forming properties of the material are destroyed by the treatment. Emulsions were not observed to form in the batch countercurrent contactors or the 2-in.-diameter extraction columns when unfiltered digested feed was used. The precipitate carried some fission product activity. It was acid-insoluble but dissolved readily in sodium hydroxide.

The "blue thorium" residue, which represented a potential loss of thorium to the process and a potential cause of plugging of the lines, because of its finely divided state, and the hydrous thorium oxides were dissolved by this treatment. This dissolution is probably a combined result of the higher salt strength, temperature, and acidity employed as compared to conditions of the regular slug dissolution procedure.

Ruthenium decontamination in the A-column was about 20 times greater with feed treated by this procedure than with an untreated feed.

4.2.1 Effect of Acid Concentration on Coagulation of Siliceous Material

A high acid concentration was necessary for precipitation of the siliceous material. A synthetic feed with the composition 3 M thorium, 1.4 M aluminum, 0.6 M HNO_3, prepared from mantle grade thorium nitrate known to contain a large amount of siliceous matter, was refluxed at atmospheric pressure. Only a small amount of precipitate was observed after 4.5 hr, and precipitation was still incomplete after 16 hr. Reflux of the same feed after its composition had been adjusted to 2.6 thorium, 1.2 M aluminum, 4 M HNO_3 caused precipitation of a noticeable amount of the siliceous matter at the end of 1.5 hr and essentially complete precipitation after 4.5 hr.

4.2.2 Change in Acidity of Feed During Evaporation

Nonradioactive dissolver solutions were evaporated at atmospheric pressure; as the thorium and aluminum concentrations increased, the acidity first increased to a maximum and then decreased to zero, or acid deficiency, when the solution had become concentrated to approximately 4 M thorium (see Fig. 4-3). The initial acidities of the solutions studied varied from 0.0 to 6.45 N and the same general result was obtained in all cases, although the curve showing the acidity rise and fall was much steeper for the initially 6.45 N acid solution.

The 6.45 N HNO_3 dissolver solution (1.0 M thorium, 0.4 M aluminum), representing a twofold excess of nitric acid, was prepared by nitric acid dissolution of thorium and aluminum according to the reaction

$$Th + 0.41\ Al + 13.1\ HNO_3 \xrightarrow{60\%\ HNO_3} Th(NO_3)_4 + 0.41\ Al(NO_3)_3 + 6.45\ HNO_3 + \text{nitrogen oxides.}$$

The other solutions were prepared from thorium nitrate tetrahydrate or by dissolving thorium metal in an approximately stoichiometric amount of nitric acid.

Since the dehydrated feed remaining at the end of the experiment was

[redacted]
Dwg No22521

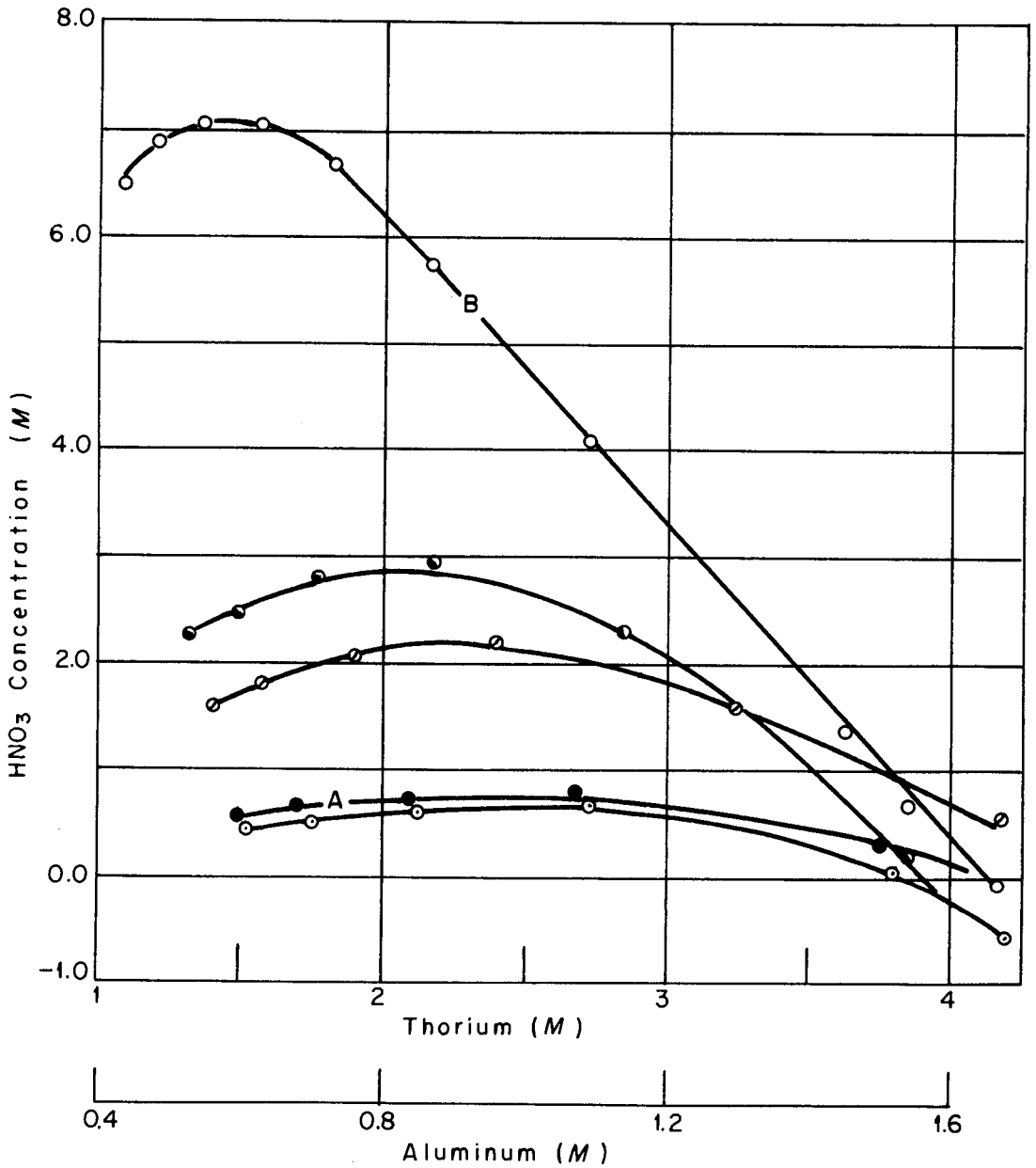

Fig. 4-3. Nitric Acid Concentration vs. Thorium and Aluminum Concentrations, Observed During Evaporation of Thorex Dissolver Solutions of Various Initial Acidities.
Curve A: Observed during evaporation of Thorex AF. Curve B: Observed during evaporation of dissolver solution obtained when twofold excess of 13 *M* nitric acid used in dissolution.

nearly neutral, it can be postulated that most of the free acid was distilled out and little water of solution remained. Assuming that the water of solution distills first and then the free acid and waters of crystallization, the high points on the curves may indicate where dehydration of the hydrous oxides and siliceous material becomes possible.

Dissolution with a twofold excess of nitric acid may be advantageous since a 4-hr evaporation cycle would bring about dehydration and the resulting solution could be adjusted to Thorex AF conditions by simple addition of water. The curve of acidity vs. thorium or aluminum concentration (see Fig. 4-3) goes through the optimum concentrations of thorium, aluminum, and acid necessary for dehydration of siliceous materials in this system.

Corrosion of Evaporator. A severe corrosion problem exists with the silicic acid—dehydration procedure which requires both high total nitrate and nitric acid concentrations. Investigation has shown that none of the stainless steels satisfactorily meet the acceptable corrosion rate of 4 to 10 mils/year (see Table 4-6 and Fig. 4-4). Type 309SCb was the best material of those studied.

4.2.3 Countercurrent Experiments on Digested Feeds

The dehydration and digestion of Thorex AF caused the formation during digestion of a yellow-colored material, presumably chromate or dichromate, which was partially extractable in the AU stream. The addition of a small amount of ferrous sulfate (0.005 M) to the AS stream prevented its extraction.

The formation of emulsions and interfacial solids in the contactors was sharply decreased by the digestion procedure used on the feed. When synthetic Thorex AF solutions (e.g., mantle grade thorium nitrate tetrahydrate) having a high silicic acid content were digested, no solids were observed after 25 equilibrations. When undigested feeds were used, solids accumulated in the contactor, causing severe emulsions and contributing to very slow phase separation. Qualitative comparison of phase separation rates when using AF's prepared from thorium slug dissolver solutions indicated that digested feeds permitted the most rapid separations, e.g., 1 min vs. about 3 min.

[redacted] Dwg. No. 22522

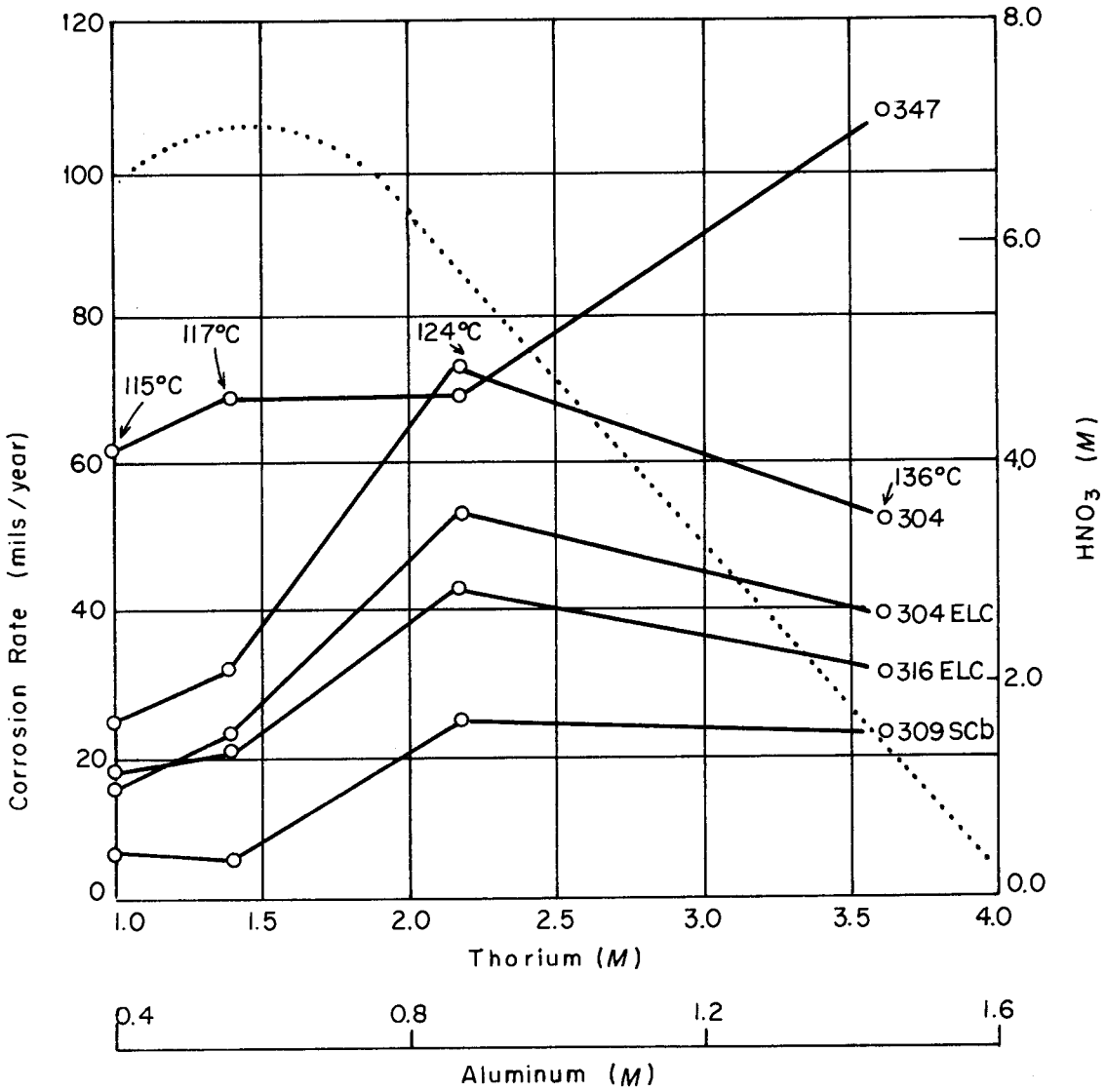

Fig. 4-4, Corrosion Rate of Unwelded Stainless Steels as Functions of Stages of Evaporation of a Solution 1.0 *M* in Thorium, 0.4 *M* in Aluminum, and 6.5 *M* in Nitric Acid.
Dotted line is reference curve to show change in nitric acid concentration.
Boiling temperatures are shown for the various corrosion test solutions.

Table 4-6

Corrosion[a] of Stainless Steels During High Temperature Reflux in Digestion Procedure (100-hr Tests)

Data for Solution 1 is plotted in Fig. 4-4

Stainless Steel (not welded and welded)	Corrosion Rate[b] (mils/year)				
	Solution 1: 1.0 M Th, 0.4 M Al, 6.5 M HNO_3, B.p. 115°C	Solution 2: 1.3 M Th, 0.5 M Al, 7 M HNO_3, B.p. 117°C	Solution 3: 2.1 M Th, 0.8 M Al, 6 M HNO_3, B.p. 124°C	Solution 4: 3.6 M Th, 1.4 M Al, 1.4 M HNO_3, B.p. 136°C	Solution 5: 3.5 M Th, 1.6 M Al, 0.0 M HNO_3, B.p. 140°C
Type 304:					
Not welded	25	32	73	52	31
Welded	27	40	131	54	30
Type 304ELC:					
Not welded	16	23	53	39	21
Welded	17	21	61	36	17
Type 316ELC:					
Not welded	18	21	43	31	19
Welded	15	25	73	51	25
Type 309SCb:					
Not welded	7	6	25	23	16
Welded	11	17	67	61	61
Type 347:					
Not welded	62	68	68	107	68
Welded	33	44	44	115	66

(a) Data obtained by J. English et al., Reactor Experimental Engineering Division.

(b) Solution 1 caused pitting of 304 and 347. Solution 2 caused pitting of all except 309SCb. Solutions 3, 4, and 5 pitted all steels tested.

4.2.4 Boiling and Freezing Points of Thorex Feed Solution During Evaporation

The approximate boiling and freezing points of synthetic Thorex feed solutions, comparable in composition to solutions obtained during the evaporation and digestion cycles, were determined (see Table 4-7) for use in design and control of the process. The boiling and freezing points were taken while agitating at atmospheric pressure during actual tests of the evaporation and digestion cycles, and the composition of the solutions was calculated from known values of initial solution, concentration ratio, and distillate acidity. The freezing points in particular must be considered approximations since it is known that impurity effects on the crystallization to thorium nitrate are significant.

Various calculated and observed data on typical evaporation procedures are given in Tables 4-8 and 9.

4.2.5 Evolution of Fluoride During Evaporation

Analysis of the distillates from one evaporation-digestion run in glass equipment indicated that about 0.1% of the fluoride present in the dissolver product was being evolved and trapped in the distillate (see Table 4-10). It is doubtful that the analysis showed the total fluoride evolved since the hydrofluoric acid formed probably attacked the glass vessel, so that some of the fluoride did not pass into the distillate. This run was made on 100 ml of synthetic Thorex dissolver solution, which was 1.5 M in thorium, 0.6 M in aluminum, 0.5 M in HNO_3, and 0.075 M in fluoride ion; 60 ml of this was distilled in 15-ml cuts.

4.2.6 Removal of Fission Products from Digested Thorex Feed Solutions by Adsorbents

Radioactive feed from a dehydration-digestion run in glass was treated batchwise with five adsorbents. A significant percentage of zirconium and niobium (see Table 4-11) was adsorbed by silica gel, filtrol, and fuller's earth. This suggests the possible use of a column or bed to adsorb this type of activity before introduction of the feed into the A-column. Data on protactinium adsorption under these conditions have not been obtained to date.

Table 4-7

Approximate Boiling and Freezing Points of Thorex Feed Solution During Digestion under Proposed Process Conditions

Initial dissolver solution: 1.5 M Th, 0.6 M Al, 0.6 M HNO_3

Concentration of Solutes[a] (M)			Boiling Point (°C)	Freezing Point (°C)
Th	Al	HNO_3		
1.5	0.6	0.6	107	<25
2.5[b]	1.0[b]	0.8[b]	120	38
3.0[b]	1.2[b]	0.79[b]	128	89
3.5[b]	1.4[b]	0.4[b]	140	115
2.8[c]	1.1[c]	3.0[c]	130	87
2.2[c]	0.88[c]	5.8[c]	118	<25

(a) Calculated from known values of initial solution, concentration ratios, and distillate acidity.

(b) Conditions observed at progressive stages of evaporation (Curve A, Fig. 4-3).

(c) Conditions comparable to proposed conditions for digestion period.

Table 4-8

Data from Typical Evaporation of Thorex Dissolver Solution, When an Essentially Stoichiometric Amount of Nitric Acid Is Used in Dissolution

Cut No.	Temperature (°C)		Residual Solution[a] Solute Concentrations (M)			Residual Solution Volume (ml)	Distillate HNO_3 Conc. (M)
	Vapor	Liquid	Th	Al	HNO_3		
0	99	107	1.5	0.6	0.55	500	---
1	102	109	1.6	0.65	0.60	460	0.05
2	103	110	1.8	0.72	0.64	420	0.09
3	104	112	2.0	0.79	0.70	380	0.14
4	105	115	2.2	0.88	0.75	340	0.25
5	106	119	2.5	1.0	0.80	300	0.45
6	109	125	2.9	1.2	0.80	260	0.91
7	113	134	3.4	1.4	0.6	220	2.2
8	116	147	4.2	1.7	-0.06	180	4.8

(a) Calculated from known values of the initial solution, concentration ratios, and distillate acidities.

Table 4-9

Data from Typical Evaporation of Dissolver Solution, When a Twofold Excess of Nitric Acid Is Used in Dissolution

Cut No.	Temperature (°C)		Residual Solution[a] Solute Concentrations (M)			Residual Solution Volume (ml)	Distillate HNO_3 Conc. (M)
	Vapor	Liquid	Th	Al	HNO_3		
0	111.5	116.5	1.1	0.4	6.45	100	---
1	115	118	1.2	0.48	6.9	90	2.93
2	117	120	1.4	0.56	7.1	80	5.05
3	118	121	1.6	0.64	7.0	70	7.25
4	119	122	1.8	0.72	6.7	60	9.40
5	119	124	2.2	0.88	5.7	50	11.20
6	120	126	2.7	1.1	4.1	40	12.35
7	120	136	3.6	1.4	1.4	30	12.20
8	120	140	3.9	1.6	0.7	28	10.65

(a) Calculated from known values of the initial solution, concentration ratios, and distillate acidities.

Table 4-10

Observed Evolution of Fluoride During Evaporation of Thorex Dissolver Solution

100 ml of synthetic Thorex dissolver solution, 1.5 M thorium, 0.6 M aluminum, 0.5 M nitric acid, 0.075 N fluoride; 60 ml of this distilled in four 15-ml cuts; final residual concentrations were ~3.6 M thorium, 1.5 M aluminum, 0.1 M nitric acid, and ~ 0.18 N fluoride.

Cut No.	Fluoride in Distillate (ppm)
1	0.80
2	0.68
3	2.98
4	11.5
Average	4.0

Table 4-11

Effectiveness of Adsorbents for Activity Removal from Thorex Digested[a] Feeds

0.1 g of adsorbent and 5 ml of digested Thorex feed agitated for 10 min; solutions centrifuged and counted.

Adsorbent	Activity Removed (% of total)	
	Zr β	Nb β
Silica gel, 70 mesh	67	38
Filtrol	65	79.8
Fuller's earth	57.5	78.5
Fisher adsorption alumina	1.8	15.7
Aluminum trihydrate	0.0	0.0

(a) Digestion carried out in glass equipment.

The amount of fission product removed was shown to be a function of the amount of adsorbent used. A synthetic Thorex solution spiked with fission products was dehydrated and digested in the presence of type 309 stainless steel turnings and treated with different amounts of adsorbent. More of both the zirconium and niobium present were removed with the larger amount of adsorbent (see Table 4-12).

Table 4-12

Adsorption of Activity on Filtrol Following Digestion in Presence of Type 309SCb Stainless Steel

Filtrol (g/liter of feed solution)	Activity Removed (% of total)	
	Zr β	Nb β
10.0	63.5	42
100.0	91.5	59.5

4.3 Ruthenium Decontamination
(R. P. Wischow)

As previously postulated (ORNL-1518, p. 9), ruthenium appears to be the limiting contaminant of thorium and uranium in the Thorex process. Ruthenium can exist in at least nine different oxidation states and in many complex species. Many of the erratic phenomena in ruthenium extraction may be charged to the variable oxidation states and equilibria in feeds of variable history and the disproportionation between these states during extraction. The extractable species of ruthenium do not presumably have a colloidal nature in the Thorex process as far as it has been determined. This assumption is based on the reproducible analytical results obtained with individual samples.

4.3.1 Isolation of Ruthenium Species

Isolation of specific ruthenium species was attempted in two runs on synthetic feed with a 16-stage batch countercurrent extraction apparatus designed to separate and concentrate species having different distribution coefficients. In one run, in which the solution developed acidity at the feed plate (X-160), the ruthenium D.C. (O/A) approached 1.1 as the stage number increased (see Table 4-13 and Fig. 4-5). This effect has been noticed in Thorex process runs, particularly in the A-column. However, when the feed stage solution remained neutral (X-162), the ruthenium D.C. (O/A) was always less than 1.0, and the presence of three predominant species, having distribution coefficients of about 0.002, 0.16, and 0.35 (see Table 4-13 and Fig. 4-5) was indicated. These differences indicate the influence of feed acidity on the types and quantities of ruthenium fractions which may be expected in the Thorex process.

Conditions in Run X-160 were similar to those in the Thorex A-column since the system was initially acidic and gradually became basic. In Run X-162 the feed ruthenium was digested (at room temperature) in a basic system, and the aqueous solution was analogous to an acid-deficient Thorex AF stream; the organic stream was neutral. Unless other factors prohibited the use of such a basic feed solution, ruthenium decontamination could probably be increased to some extent by digesting the feed in a basic system and adjusting the scrub flow rates. However, development of other head-end treatments (see Sect. 4.3.2), to give higher decontamination factors, following acid digestion would eliminate the need for drastic changes in flow conditions.

The feed, scrub, and organic streams used in these runs had been previously equilibrated with respect to thorium, aluminum, and acid so that essentially only the ruthenium would be transferred through the system. The aqueous feed was equivalent in composition to equilibrium feed plate conditions of the Thorex A-column. (The accidental presence of a small amount of nitric acid in the organic phase in Run X-160 caused the feed plate to become acidic as the run progressed.) The aqueous scrub and organic were equivalent in composition to equilibrium solutions of the scrub section in the A-column. The feed was placed in the first stage, and equivalent volumes of scrub solution were placed in the last 15 stages.

[redacted]
Dwg. No 22523

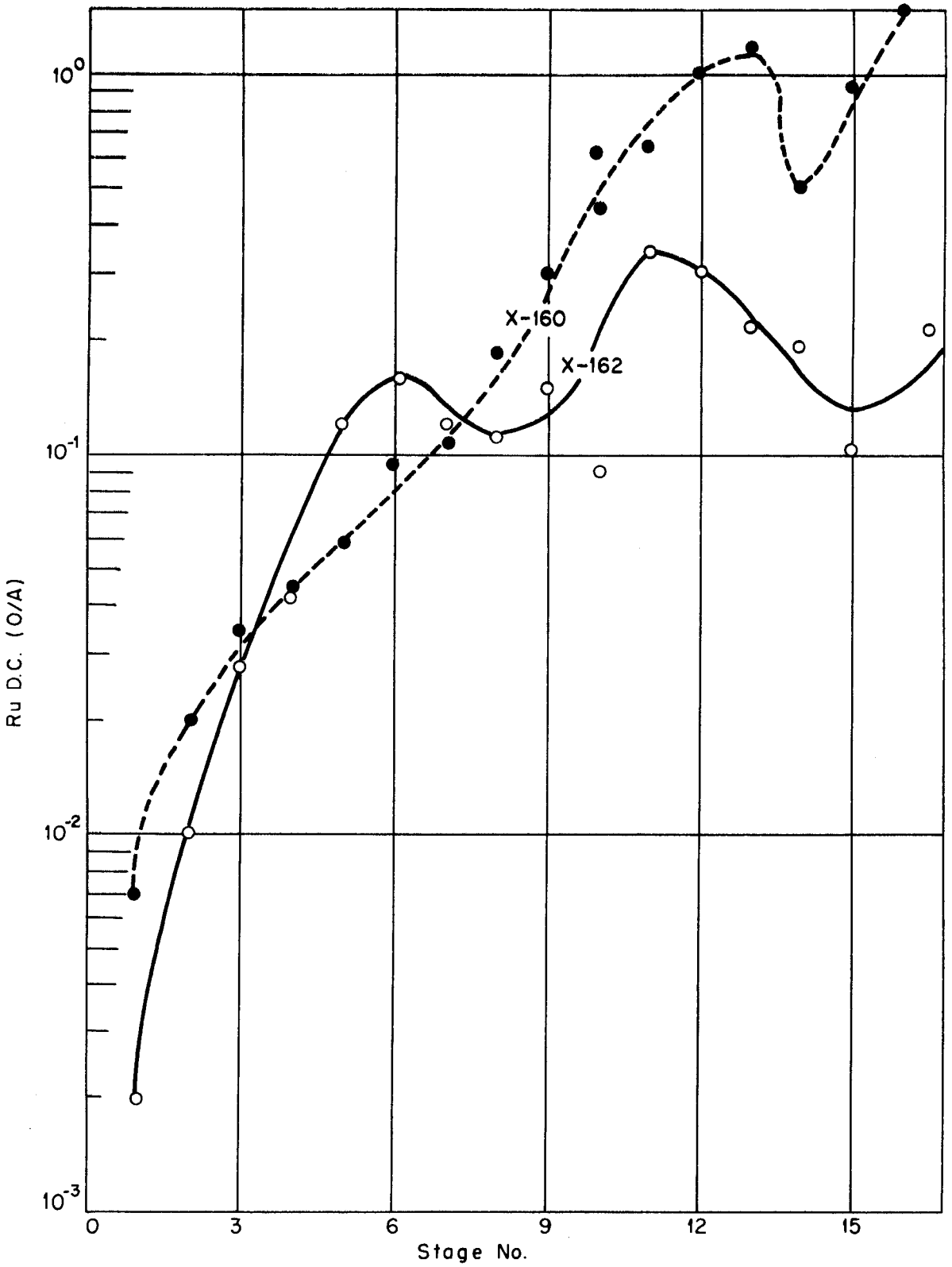

Fig. 4-5. Separation of Ruthenium Species: Ruthenium D.C.(O/A) vs. Stage Number in Batch Countercurrent Extraction Apparatus.

Table 4-13

Distribution of Ruthenium Species in Aqueous and Organic Phases of Extraction (16-stage) Apparatus

(See Sect. 4.3.1 for conditions and operation of apparatus)

Stage	Organic			Aqueous			D.C. (O/A)	
	Thorium (g/liter)	HNO_3 [a] (M)	Ru β (c/m/ml)	Thorium (g/liter)	HNO_3 [a] (M)	Ru β (c/m/ml)	Ru β	Thorium
Run X-160 (feed stage became acid)								
1	91	0.04	5.7×10^4	70	+0.25	7.8×10^6	0.007	1.3
2	98	-0.007	2.4×10^4	109	-0.36	1.1×10^6	0.022	0.9
3	94	-0.02	9.0×10^3	130	-0.62	2.6×10^5	0.035	0.7
4	92	-0.02	3.6×10^3	124	-0.66	8.0×10^4	0.045	0.7
5	88	-0.03	2.1×10^3	110	-0.66	3.4×10^4	0.062	0.8
6	83	-0.02	1.4×10^3	106	-0.69	1.4×10^4	0.097	0.8
7	79	-0.03	9.8×10^2	99	-0.69	9.0×10^3	0.109	0.8
8	76	-0.03	9.8×10^2	96	-0.70	5.2×10^3	0.187	0.8
9	74	-0.03	1.1×10^3	89	-0.71	3.6×10^3	0.298	0.8
10	73	-0.03	1.3×10^3	82	-0.71	3.6×10^3	0.435	0.9
11	74	-0.03	1.9×10^3	71	-0.71	2.9×10^3	0.642	1.0
12	74	-0.03	2.6×10^3	91	-0.71	2.7×10^3	0.99	0.8
13	74	-0.04	2.6×10^3	91	-0.69	2.3×10^3	1.14	0.8
14	74	-0.03	8.9×10^2	91	-0.70	2.0×10^3	0.44	0.8
15	74	-0.04	1.4×10^3	91	-0.70	1.6×10^3	0.92	0.8
16	72	-0.03	1.7×10^3	90	-0.70	1.1×10^3	1.5	0.8

Table 4-13 (Cont.)

Stage	Organic			Aqueous			D.C. (O/A)	
	Thorium (g/liter)	HNO_3 (a) (M)	Ru β (c/m/ml)	Thorium (g/liter)	HNO_3 (a) (M)	Ru β (c/m/ml)	Ru β	Thorium
Run X-162 (feed stage remained neutral)								
1	115	-0.002	2.2×10^4	144	-0.58	1.0×10^7	0.002	0.8
2	113	-0.01	4.3×10^3	100	-0.58	3.4×10^5	0.013	1.1
3	109	-0.01	1.2×10^3	139	-0.60	4.3×10^4	0.028	0.8
4	101	-0.02	3.8×10^2	120	-0.62	9.0×10^3	0.042	0.8
5	104	-0.03	5×10^2	117	-0.62	3.6×10^3	0.14	0.9
6	96	-0.03	3.6×10^2	106	-0.62	2.2×10^3	0.16	0.9
7	84	-0.03	2.2×10^2	100	-0.56	2.2×10^3	0.10	0.8
8	68	-0.04	1.4×10^2	96	-0.64	1.7×10^3	0.12	0.7
9	87	-0.04	2.6×10^2	94	-0.62	1.6×10^3	0.17	0.9
10	76	-0.04	1.4×10^2	94	-0.60	1.5×10^3	0.09	0.8
11	59	-0.01	5.2×10^2	92	-0.62	1.5×10^3	0.34	0.6
12	66	-0.01	4.8×10^2	92	-0.60	1.6×10^3	0.29	0.7
13	70	-0.03	3.2×10^2	92	-0.60	1.4×10^3	0.23	0.8
14	48	-0.002	2.8×10^2	95	-0.60	1.5×10^3	0.19	0.5
15	41	-0.002	1.4×10^2	94	-0.60	1.3×10^3	0.11	0.4
16	54	-0.005	3.2×10^2	94	-0.60	1.4×10^3	0.24	0.6

(a) The minus sign indicates acid deficiency.

The solvent and the feed containing ruthenium were then equilibrated at a volume ratio of 1/1 in the first stage of the system. The organic phase was separated and added to the first scrubbing stage, and fresh solvent was added to the extraction stage containing the initial feed solution. This procedure was repeated until all 16 stages were filled with organic and aqueous solutions. (These conditions permit complete extraction from the feed stage of all species having D.C.'s (O/A) of 1.0 or greater and distribute such species throughout the scrub section, concentrating them at a specific scrub stage characteristic of their distribution coefficients. Those species with D.C.'s (O/A) of less than 1.0 move only a slight distance past the feed plate and will concentrate at a given stage. A degree of purification of fractions having significantly different distribution coefficients is thus effected.) Samples of both phases were taken and analyzed immediately after the run was completed.

Macro ruthenium nitrate, at equilibrium with Ru^{106} tracer, was added to the feed to permit visual observation of color changes and/or qualitative observation of individual valence states, if possible, during the extraction. Essentially no color was observed in the last 14 stages. The first-stage solution was dark brown owing to the presence of Ru^{3+} and Ru^{4+}. It is not known whether the macro ruthenium and the tracer ruthenium had reached true equilibrium.

4.3.2 Head-End Treatments

Studies of an AF evaporation-digestion procedure (see Sect. 4.2) designed primarily to clarify the dissolver solutions have indicated that the bulk of the extractable ruthenium fraction is converted to a less extractable form during the operation when the digestion is carried out in the presence of type 309 stainless steel (see Tables 4-14 and 15). Ruthenium decontamination factors of the same order as obtained with the HIO_4-HCOOH method (ORNL-1518, p. 9) were observed. With undigested feed a D.C. (O/A) of greater than 1.0 was observed in the eighth scrub stage. With the digested feed a D.C. (O/A) of less than 1.0 and usually less than 0.6 was found. This suggests that marked changes occurred during the digestion step to affect the organic-aqueous

Table 4-14

Effect of Head-End Treatments on Decontamination:
Summary of Fission Product Decontamination Factors

Run No.	Feed Treatment	Final AF Gross β (c/m/ml)	Decontamination Factors				
			Gross β	Ru β	Zr β	Nb β	TRE β
X-141	None	1.89×10^8	365	20	9.01×10^5	3.14×10^4	5.3×10^5
X-169	None	8.68×10^7	95	8	6×10^3	5×10^4	1.9×10^6
X-185	None	1.27×10^8	510	35	1.0×10^4	1.9×10^3	1.1×10^5
X-175	Digestion	9×10^7	782	57	9.7×10^3	1×10^4	2.1×10^5
X-179	Digestion in presence of type 309 stainless steel	3.43×10^8	2050	296	1.3×10^4	2.9×10^3	1.6×10^5
X-174	Digestion in presence of excess silicic acid	7.5×10^7	4250	278	5.2×10^4	1.6×10^3	9.5×10^4
X-177	Digestion in presence of excess silicic acid	8.25×10^7	1450	67	7.2×10^3	1.1×10^3	1.4×10^6
X-181	Digestion in presence of silica gel	1.5×10^8	560	71	2×10^3	4.7×10^3	1.3×10^5
X-182	Digestion followed by silica gel—Filtrol column	3.24×10^8	780	82	4.6×10^3	4.2×10^3	8.6×10^5
X-171	Head-end treatment with HIO_4, HCOOH, $Na_2Cr_2O_7$	8.44×10^7	950	48	1.5×10^4	3.7×10^3	2.6×10^5
X-186	Digestion in presence of Duriron	1.41×10^8	580	77	1.32×10^4	4.5×10^3	4.9×10^5
X-183	No feed treatment; HIO_4 in scrub	3.14×10^8	566	61	2×10^3	8.2×10^3	5.4×10^5

Table 4-15

Summary of A-Column D.C.'s (O/A) for Ruthenium and Gross Beta at the Feed Plate, Extraction Section, and Scrub Section following Various Head-End Treatments

Run No.	Treatment	Final AF Gross β (c/m/ml)	Distribution Coefficients (O/A)					
			8th Scrub Stage		Feed Plate		5th Extraction Stage	
			Ru β	Gross β	Ru β	Gross β	Ru β	Gross β
X-169	None	8.68×10^7	1.03	1.05	0.19	0.026	0.016	0.18
X-175	Digestion	9×10^7	0.45	0.45	0.29	0.045	0.007	0.15
X-179	Digestion in presence of type 309 stainless steel	3.43×10^8	0.60	0.60	0.13	0.03	0.001	0.16
X-174	Digestion in presence of excess silicic acid	7.5×10^7	0.25	0.24	0.06	0.04	0.004	0.13
X-177	Digestion in presence of excess silicic acid	8.25×10^7	---	0.9	0.27	0.05	0.005	0.11
X-181	Digestion in presence of silica gel	1.5×10^8	0.45	0.58	0.17	0.03	0.012	0.13
X-182	Digestion followed by silica gel—Filtrol column	3.24×10^8	0.45	0.43	0.19	0.03	0.007	0.32
X-171	Head-end treatment with HIO_4, HCOOH, $Na_2Cr_2O_7$	8.44×10^7	0.63	0.6	0.14	0.03	0.013	0.18
X-183	No feed treatment; HIO_4 in scrub	3.14×10^8	0.86	0.91	0.03	0.02	0.019	0.20

distribution of the ruthenium. The distribution of the various fission products following the digestion procedure is given in Table 4-16.

It was previously reported (ORNL-1518, p. 9) that the major distribution coefficients of the ruthenium in the A-column were 0.003 and 1.0 for the extraction and scrub sections, respectively. Present data indicate that other species are present as a result of different AF histories. The prominent ruthenium distribution coefficient in digested feed appears to be about 0.002 in the extraction section, with 0.25 and 0.5 being observed in the scrub section. The species having a D.C. (O/A) of about 1.0, observed generally with untreated feeds, appears to be absent.

Use of present A-column flow ratios will not permit decontamination from ruthenium species having D.C.'s greater than 0.2. Thus it can be seen that the present AF digestion operation is not entirely satisfactory as a method for decontamination without significant increases of the AS/AX ratio.

Unexplained variations are apparent in the experimental data throughout all the ruthenium studies. It appears that the rate of disproportionation between the extractable and nonextractable species varies from run to run and experimental control is insufficient.

4.3.3 Effects of Additives in the Scrub Section

A number of oxidizing and reducing agents have been added to the scrub solution to observe their effects on the ruthenium distribution coefficients. No definite benefits of most of the additives were observed. The additives were reasonably strong oxidizing or reducing agents, so it appeared that the extractable species was somewhat stable (see Table 4-17). The use of $Na_2S_2O_4 \cdot 2H_2O$ decreased the ruthenium distribution coefficient. As the concentration of this reagent in the scrub stream increased, the ruthenium D.C. (O/A) decreased (see Fig. 4-6). Potassium permanganate appeared to offer some promise, but subsequent data showed the effect to be irreproducible.

The highly extractable ruthenium species (D.C. > 1.0) has been considered to be a nitrite complex of ruthenium, possibly $Ru(NO_3)_3NO$, and has been shown in recent experiments with macro ruthenium to be decomposed by such reducing

[redacted]
Dwg. No. 22524

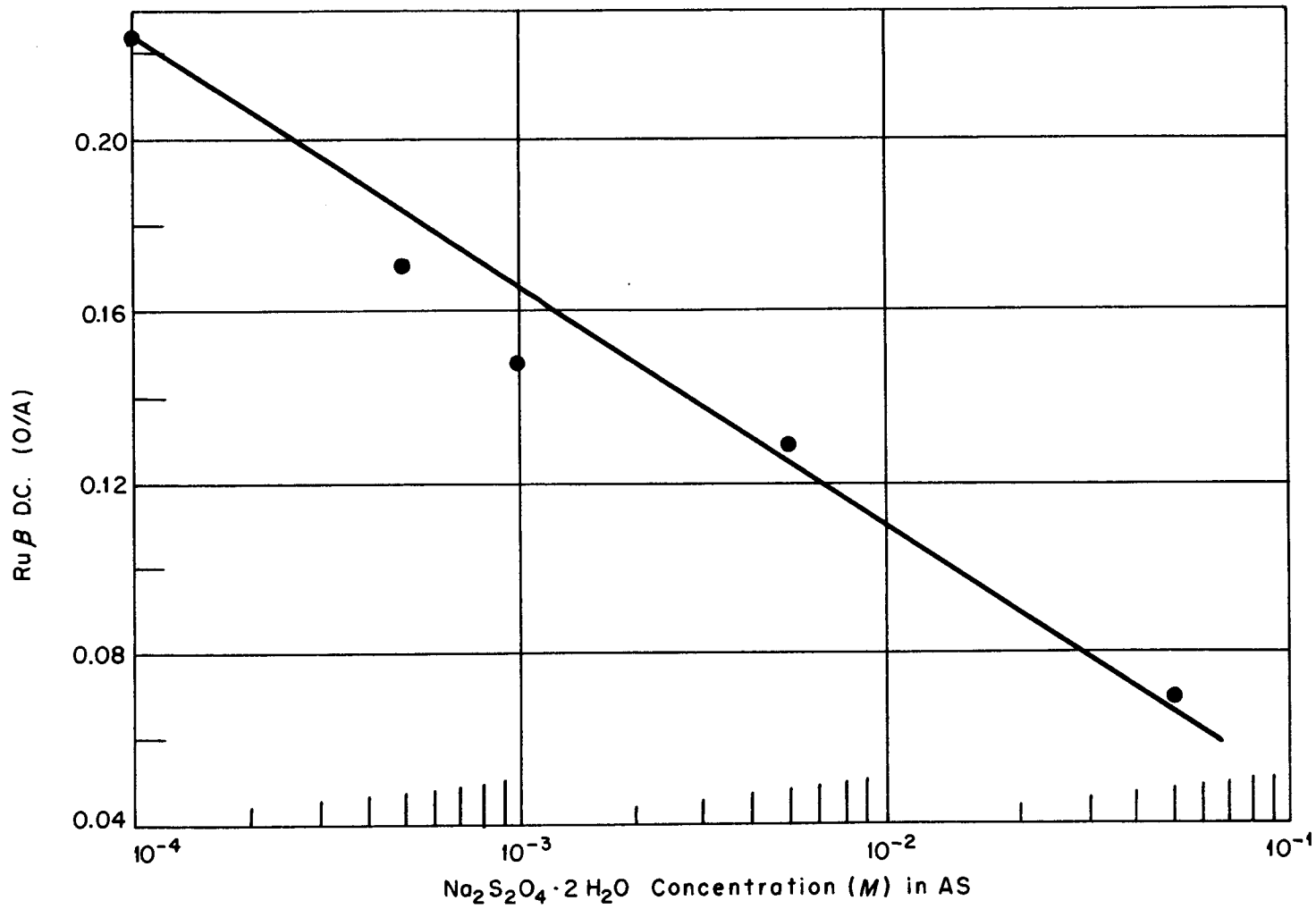

AU/AS flow ratio: 5.0
Contact time: 1 min.

Fig. 4-6 Ruthenium D.C. (O/A) in the AU Stream as a Function of Sodium Hydrosulfite Concentration in the AS Stream.

Table 4-16

Fission Product Distribution in A-Column:
Typical Countercurrent Data When Using the AF Digestion Procedure

AF contained fission products as follows, in β c/m/ml: Ru, 7.60×10^6; Zr, 5.5×10^6; Nb, 9.5×10^5; TRE, 6.3×10^7.

Stage	Fission Product	β Activity (c/m/ml) Organic	β Activity (c/m/ml) Aqueous	D.C. (O/A)	E.F. (O/A)
8S	Ru	2.52×10^4	5.56×10^4	0.454	2.27
	Zr	117	---	---	---
	Nb	~18	---	---	---
	TRE	~56	734	0.076	0.38
6S	Ru	3.11×10^4	2.76×10^5	0.113	0.565
	Zr	88	1.93×10^3	0.046	0.23
	Nb	28	377	0.074	0.37
	TRE	662	1.39×10^4	0.0475	0.238
4S	Ru	1.29×10^5	1.26×10^6	0.102	0.51
	Zr	438	8.72×10^3	0.05	0.25
	Nb	~67	1.31×10^3	0.05	0.25
	TRE	1.30×10^4	3.33×10^5	0.04	0.20
2S	Ru	5.5×10^5	8.42×10^6	0.065	0.325
	Zr	2.53×10^3	9.53×10^4	0.027	0.135
	Nb	488	1.73×10^4	0.028	0.14
	TRE	3.04×10^5	9.73×10^6	0.031	0.155
1E	Ru	2.67×10^6	9.07×10^6	0.294	0.735
	Zr	5.16×10^4	3.31×10^6	0.016	0.04
	Nb	2.44×10^3	6.99×10^5	0.004	0.01
	TRE	9.20×10^6	2.58×10^8	0.036	0.09

Table 4-16 (Cont.)

Stage	Fission Product	β Activity (c/m/ml)		D.C. (O/A)	E.F. (O/A)
		Organic	Aqueous		
3E	Ru	1.80×10^5	3.12×10^6	0.058	0.145
	Zr	3.32×10^3	3.04×10^6	0.001	0.0025
	Nb	~ 103	5.80×10^5	1.8×10^{-4}	4.5×10^{-4}
	TRE	2.42×10^7	3.48×10^7	0.695	1.74
5E	Ru	2.0×10^4	3.07×10^6	0.007	0.0175
	Zr	869	2.99×10^6	2.9×10^{-4}	6.25×10^{-4}
	Nb	~ 22	5.55×10^5	---	---
	TRE	1.86×10^6	3.54×10^6	0.525	1.31

Table 4-17

Effect of AS Additives on Distribution Coefficient of Extractable Ruthenium

Scrub made ~0.05 M in each additive; scrub/organic ratio = 1/5; batch tests performed immediately with the AU streams from a countercurrent run.

Additive	Organic (c/m/ml)		Aqueous (c/m/ml)		D.C.'s (O/A)	
	Gross β	Ru β	Gross β	Ru β	Gross β	Ru β
$Ce(NO_3)_3$	2.98×10^4	3.22×10^4	2.25×10^4	2.34×10^4	1.33	1.37
$Co(NO_3)_2$	3.63×10^4	3.75×10^4	3.24×10^4	3.33×10^4	1.12	1.12
H_2O_2	3.82×10^4	4.12×10^4	1.99×10^4	1.98×10^4	1.92	2.08
$Mn(NO_3)_2$	4.12×10^4	3.84×10^4	3.41×10^4	3.60×10^4	1.21	1.07
$HgNO_3$	4.87×10^4	4.81×10^4	7.51×10^4	4.34×10^4	0.65	1.11
$Ni(NO_3)_2$	5.28×10^4	4.76×10^4	4.21×10^4	4.48×10^4	1.25	1.06
$MoO_3 \cdot 2H_3PO_4$	4.76×10^4	4.64×10^4	6.06×10^4	6.42×10^4	0.79	0.72
$KMnO_4$	3.10×10^4	1.08×10^4 (a)	5.46×10^4	5.58×10^4	0.57	0.19
$RuCl_3$	4.47×10^4	3.70×10^4	5.03×10^4	4.95×10^4	0.89	0.75
$H_8SiW_{12}O_{42}$	4.85×10^4	3.20×10^4	3.86×10^4	3.74×10^4	1.25	0.85
CH_3OH	6.47×10^4	6.22×10^4	5.87×10^4	5.97×10^4	1.10	1.04
$N_2H_4 \cdot H_2SO_4$	5.88×10^4	5.14×10^4	6.13×10^4	6.22×10^4	0.96	0.83
HCOOH	5.73×10^4	5.40×10^4	5.42×10^4	5.84×10^4	1.06	0.93
$NH_2OH \cdot HCl$	6.65×10^4	6.32×10^4	5.68×10^4	5.90×10^4	1.17	1.07
None	5.70×10^4	5.47×10^4	5.63×10^4	5.43×10^4	1.01	1.01

(a) Presumably an error. Not reproduced in subsequent tests.

agents as $Na_2S_2O_4 \cdot 2H_2O$, $SnCl_2$, and $TiCl_3$. However, most reducing agents appear unfeasible as process additives owing to adverse effects involving precipitations and formation of interfacial solids.

4.3.4 Disproportionation Rate of the Extractable Ruthenium Species

The rate of disproportionation of the extractable ruthenium fractions (distribution coefficients of 0.6 to 1.2) in the Thorex AU stream were investigated. The D.C.'s (O/A) were observed to decrease at a rate of about 0.4 unit per hour during the first 2 hr (see Fig. 4-7). The distribution coefficient at final equilibrium has not been determined; however it is suspected that the value becomes less than 0.1. The above data, along with factors discussed in Sect. 4.3.1 may permit the conclusion that acid-deficient conditions in the AS stream promote formation of nonextractable ruthenium species, but process contact times limit the full advantage of the effect to ruthenium decontamination. Ways and means of utilizing this effect, e.g., by the use of an acid-deficient AF stream, will be further considered.

4.4 Silica Gel Adsorption of Protactinium from the AP Stream (M. R. Bennett and S. S. Brandt)

Difficulties arising from interferences of unknown orgin were reported in ORNL-1518, p. 17, to limit protactinium adsorption on silica gel. Although satisfactory solution of these difficulties has not been accomplished, certain evidence has been derived from recent experiments to permit closer evaluation of the adsorption mechanism. Some impurities found at significant concentrations in the thorium slug dissolver solutions are now known to inhibit the protactinium adsorption strongly.

For example, a significant contribution of the elements niobium, iron, chromium, and nickel from the thorium slugs and their aluminum jackets was discovered. Table 4-18 records the observed relative contributions of these elements by (1) the thorium metal, (2) the aluminum jackets, and (3) nitric acid corrosion of the stainless steel dissolver, etc. Evidence presented in the following discussions indicates that niobium, ferric, and Cr^{3+} ions all interfere with the protactinium adsorption.

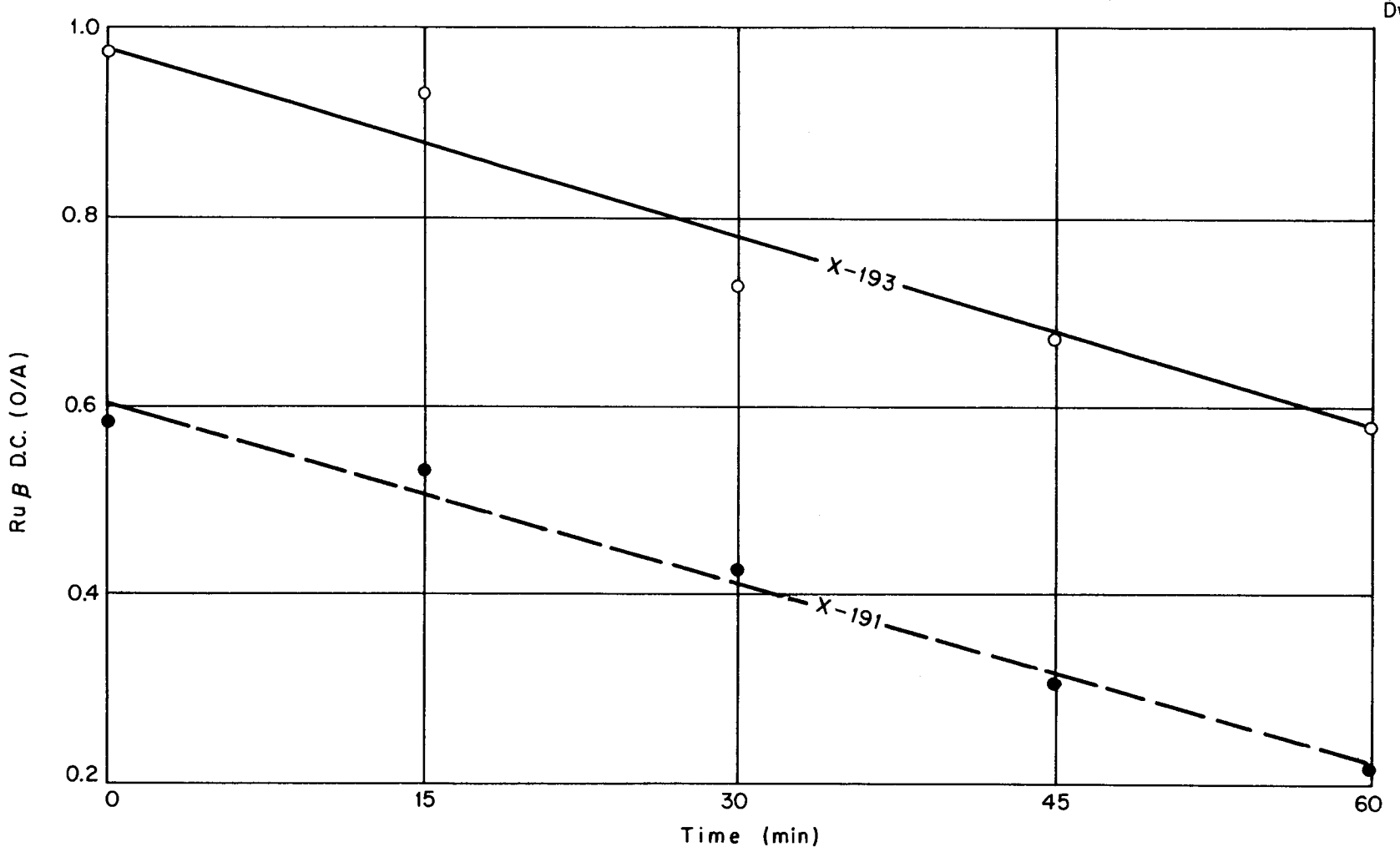

AU/AS ratio: 5.0
Contact time: 1 min

Fig. 4-7. Disproportionation of the Extractable Ruthenium Species: Ru β Distribution Coefficient as a Function of the Holdup Time in the AU Stream.

Table 4-18

Analytical Data Showing the Contribution of Thorium Metal, Aluminum Jacket, and Corrosion to the Presence of Fe, Nb, Cr, Ni, and Zr in Thorex AF Solutions

Element	Amount in AF Solution (ppm)				
	Total (1.5 M Th, 0.6 M Al)	From Th Metal (1.5 M soln)	From Al Jacket (0.6 M soln)	Total Slug + Jacket (Calcd)	From Corrosion[a] (Calcd)
Fe	324.0	90.0	16.2	106.2	218.2
Cr	56.0	1.2	1.3	2.5	53.5
Ni	50.5	7.5	2.1	9.6	40.9
Zr	---	4.4	4.7	9.1	---
Nb	216.0	135.0	150.0	285.0	---

(a) The ratio of Fe to Cr to Ni, calculated from the values in this column, which is 69 to 17 to 13, compares roughly to the composition of type 309 stainless steel.

[redacted]

4.4.1 Batch Method for Scouting Experiments (S. S. Brandt)

The evaluation of effects of test conditions on adsorption of protactinium on silica gel has been slow owing to the time required for preparing and operating adsorption columns. A new testing method has been found which gives in a few hours results comparable with those obtained in continuous column runs for materials of varying histories (see Table 4-19). The method consists in shaking 0.1 g of 70-mesh silica gel with 10 ml of test solution, centrifuging, and analyzing the supernatant. The total time required is about 1 hr. Comparable data from column runs would be obtained only after 30 to 200 column volumes of feed had passed through the adsorption column, with usually 2 to 5 working days being required. While the new method will serve to eliminate unpromising conditions, confirmatory column runs should be made under conditions that appear promising.

Table 4-19

Comparison of Results Obtained in Column Runs and Batch Runs

New method: 0.1 g of 70-mesh silica gel shaken with 10 ml of test solution and centrifuged (batch process).
Old method: 30 to 200 column volumes of test solution passed through a silica gel column (continuous process).

Test No.	Pa Retention (%)	
	Shaking and Centrifuging	Column Run
1	98.8	96.7
2	0	0
3	0	0 - 6
4	5.5	3
5	10	<27

4.4.2 Variables Affecting Adsorption
(M. R. Bennett and A. T. Gresky)

The presence of certain impurities in the metal dissolver solution was suspected to contribute to inhibition of protactinium adsorbability on silica gel. Synthetic AP streams have been spiked with various concentrations of many materials, both suspect and otherwise, in order to ascertain the nature of the causes for adsorption failure. Effects of tracer history and suspected slow equilibria of a polymerization mechanism have also been briefly investigated.

Effects of Certain Impurities as Functions of Concentrations. Synthetic AP solutions (0.67 M in aluminum, 0.15 M nitric acid deficient) were spiked with Pa^{233} tracer and variable concentrations of individual materials suspected or reported to affect protactinium adsorbability on silica gel. The batch method described in Sect. 4.4.1 was used to determine the effects of these materials on protactinium adsorption. Niobium, ferric ion,* chromic ion, hydrogen peroxide, tartaric acid, citric acid, magnesium, and calcium inhibited adsorption (see Figs. 4-8 and 9 and Table 4-20). Chromate ion at concentrations of about 0.1 M increased adsorption.** Beryllium had practically no effect.

Sulfate and phosphate ions reduced the inhibition due to niobium (see Fig. 4-8) but had no effect on the marked inhibition by ferric ion, but there are indications that chromate ion at proper concentrations will reduce the inhibition due to ferric ion (see Fig. 4-10). It became apparent during the chromate study that protactinium was carried on a chromate precipitate which had a maximum insolubility at a chromate concentration of 0.06 M in a synthetic AP stream of the composition 0.67 M aluminum, 0.12 M nitric acid deficiency. The chromate precipitate redissolved when the concentration

---

* No Fe^{3+} was added to the synthetic AP stream at point A in Fig. 4-9; however, inadvertent addition of trace amounts of Fe^{3+} might account for the low value of 57% adsorption.

** The low adsorption of protactinium (see Fig. 4-9) in the vicinity of 10^{-3} M $CrO_4^{=}$ (as added) may possibly be accounted for by partial reduction to Cr^{3+} by the action of low concentrations of unknown reducing agents.

[redacted]

[redacted]
Dwg No 22526

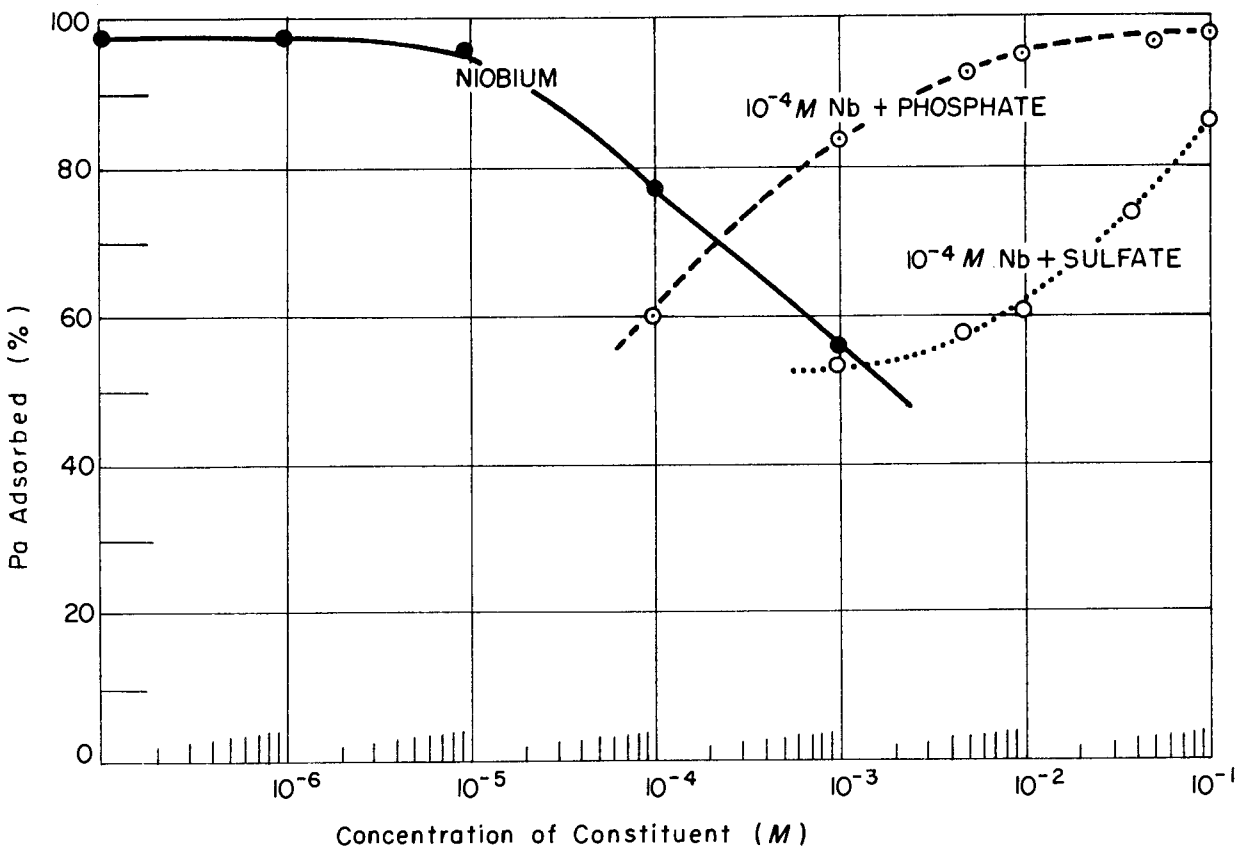

Fig. 4-8. Effect of Niobium on Adsorption of Protactinium on Silica Gel from Synthetic Thorex AP Streams.

[redacted]

Dwg No22527

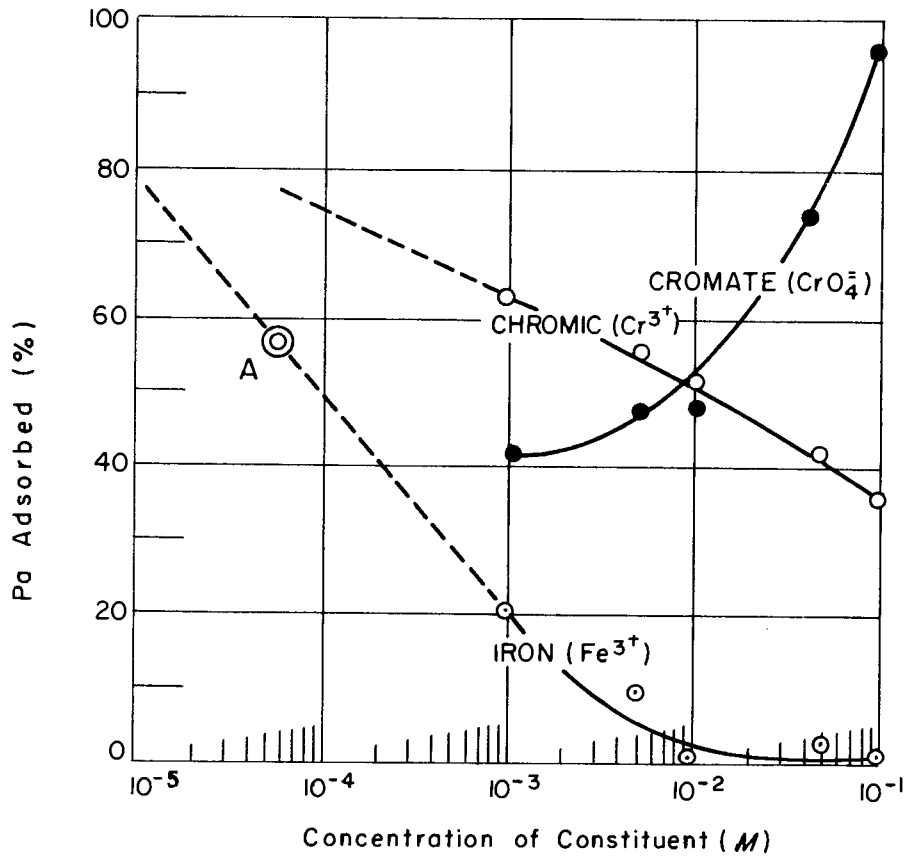

Fig. 4-9. Effect of Iron and Chromium on Adsorption of Protactinium on Silica Gel from Synthetic Thorex AP Stream.

[redacted]

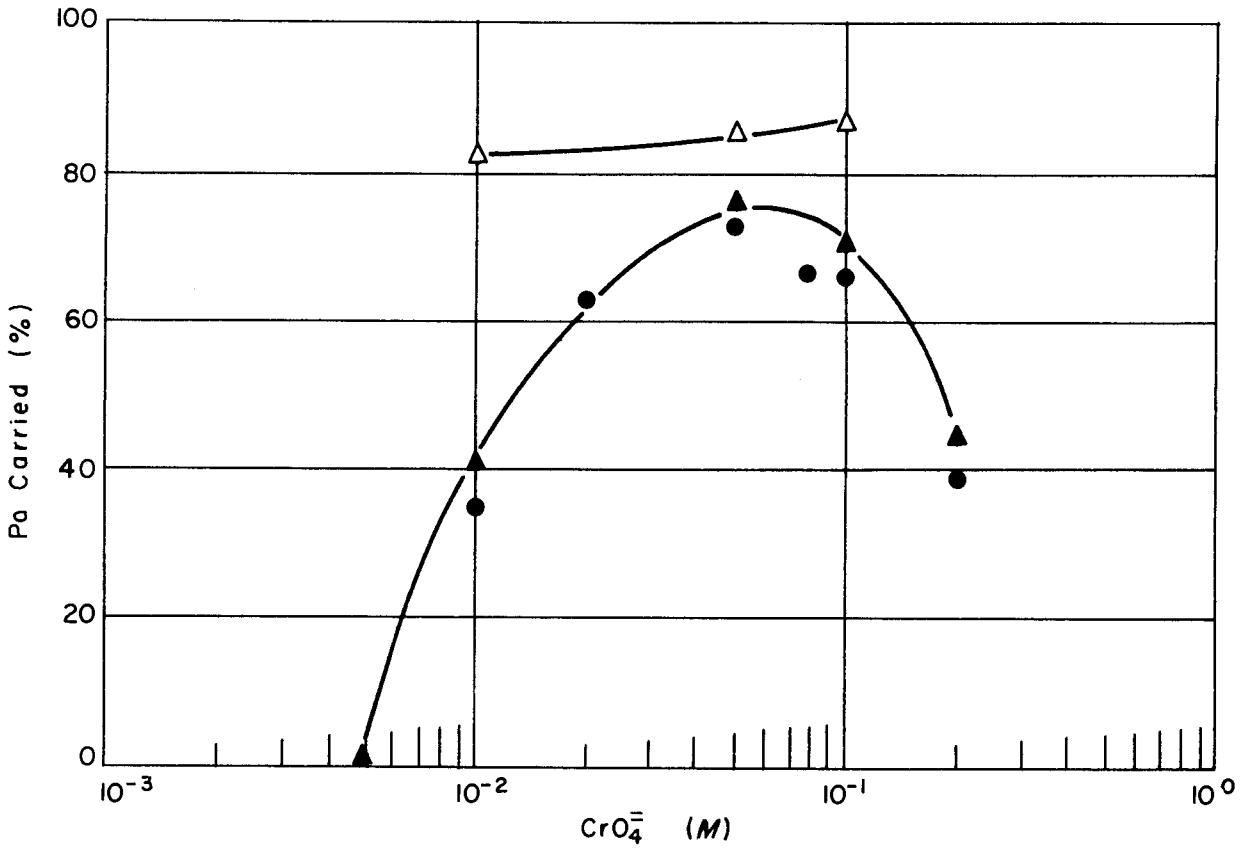

● ▲ No silica gel

△ 200 mg of silica gel per 10ml

Fig. 4-10. Effect of $CrO_4^{=}$ in Presence of 0.003*M* Fe^{3+} (0.118 *N* acid-deficient aluminum nitrate nonahydrate) on Adsorption and Carrying of Protactinium from Synthetic Thorex AP Solution.
All solutions were centrifuged for 15 min before counting.

Table 4-20

Effect of Various Materials on Silica Gel Adsorption of Pa^{233} from Thorex AP Solutions Containing Ferric Ion

Solution: 0.55 M $Al(NO_3)_3$, 0.2 N HNO_3-deficient, 0.003 M Fe^{3+},[a] Pa^{233} tracer; 20 ml was contacted with 200 mg of ~70-mesh silica gel for 15 min and then centrifuged for 10 min.

Additive	Concentration (M)	Pa^{233} Adsorbed (%)		
		Control[b]	Fe^{3+} + Additive	Additive Alone
$CrO_4^{=}$[c]	0.05	82	86	---
IO_4^{-}[c]	0.01	75	30	---
	0.05	75	96	---
$C_2O_4^{=}$	0.05	73	13	---
SO_4^{2-}	0.01	81	17	---
	0.1	81	43	---
PO_4^{3-}	0.01	88	4	---
	0.05	88	11	---
Citric acid	0.01-0.1	80	< 2	---
Tartaric acid	0.01-0.1	80	< 2	---
H_2O_2	0.01-0.05	80	~ 10	---
Mg^{2+}	0.05	87	10	---
	0.2	87	17	---
Ca^{2+}	0.05-0.2	87	~ 15	---
Be^{2+}	0.005-0.05	82	---	83

(a) Protactinium adsorption < 2% owing to Fe^{3+}.
(b) Contained neither Fe^{3+} nor additive.
(c) Precipitates formed.

was increased to 0.2 M $CrO_4^{=}$ (see Fig. 4-10). This chromate precipitation will be investigated as a possible substitute for the silica gel adsorption method. The precipitate is suspected to be a chromate salt of aluminum owing to the equivalent stoichiometry of the nitric acid deficiency and the chromate concentration observed at the point of highest insolubility. Solubility in excess $CrO_4^{=}$ is suspected to result from complexation.

Effects of Tracer History and Polymerization. Among the variables affecting the chemical and physical behavior of tracer protactinium is its history. Analysis of the tracer history problem is complicated by the dearth of fundamental knowledge of radiocolloid behavior in complex nitrate systems.

Evidence of somewhat unusual effects of digestion in highly acid-deficient and highly acidic nitrate systems has been observed (see Fig. 4-11). An apparent slow rate of change of species from nonadsorbable forms to adsorbable forms, and vice versa, as a function of acidity suggests that colloidal and ionic equilibria will interfere with reproducibility in adsorption techniques. These experiments were carried out on Pa^{233} that had aged for six months in a solution of the composition 1.8 M aluminum, 0.9 M nitric acid deficiency, 0.08 M fluoride ion, and then been adjusted to 1.0 M nitric acid with 16 M nitric acid. The steps were: (1) The protactinium was extracted into diisobutyl carbinol and stripped with 0.1 M sodium fluoride. (2) The strip was adjusted to 7 M nitric acid and the protactinium was stripped from it. (3) This strip was adjusted to 7 M nitric acid and was permitted to age for 20 days, during which time aliquots were used for experiments at the intervals indicated. The percentage of protactinium adsorbed following steps 1 and 2 was measured and found to be less than 10%. Solution conditions during adsorption studies were 0.67 M aluminum, 0.12 M nitric acid deficiency. Nonadsorbable fractions were shown by scintillation counting to be unquestionably Pa^{233}.

Since the behavior of macro amounts of protactinium may be quite different from that of tracer amounts, no definite decision can be reached on a Pa^{233} recovery process until full-scale Thorex demonstrations can be provided in the pilot plant. It now appears that adsorption or carrier

[redacted]
Dwg No 22529

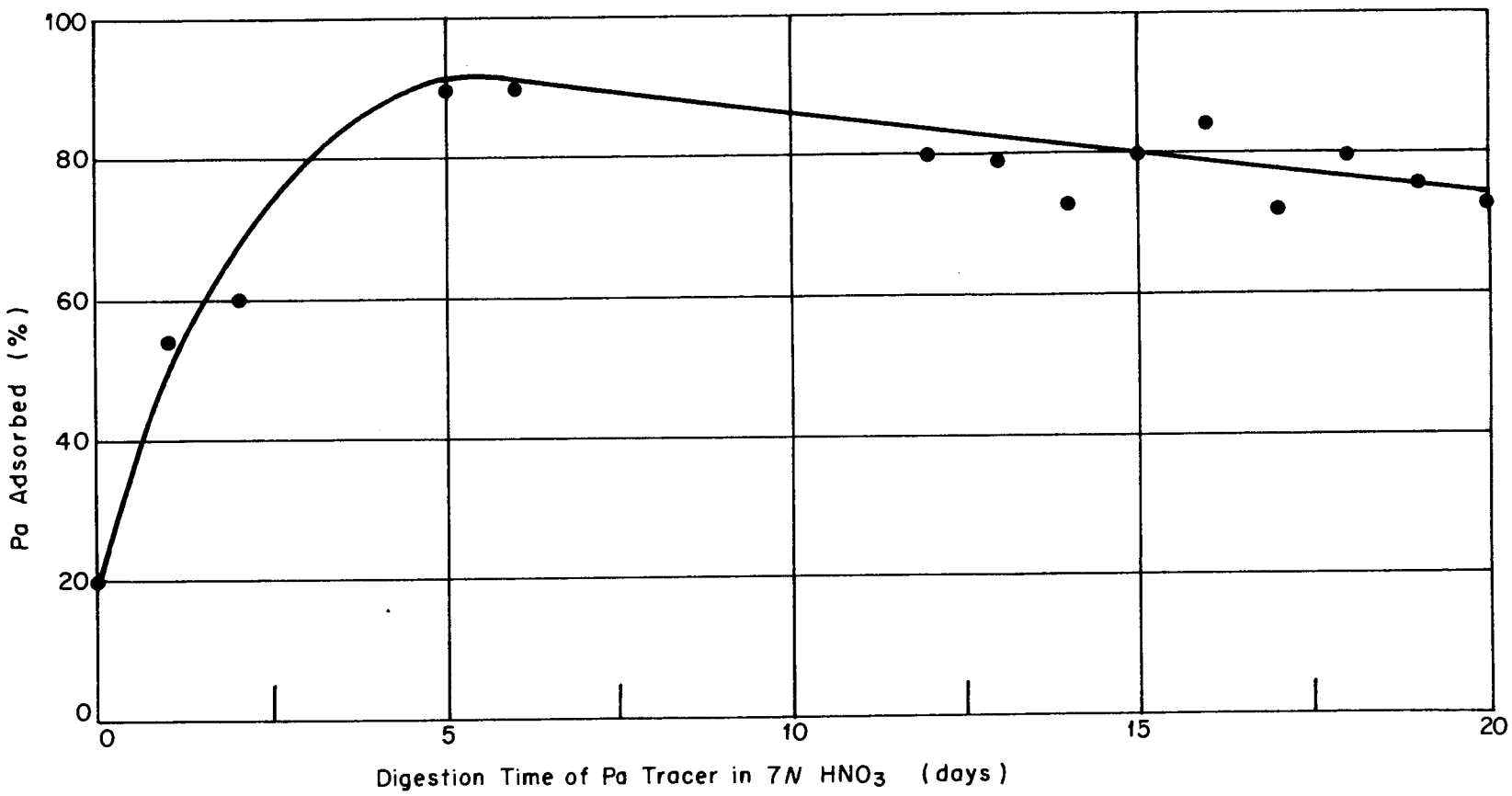

Fig. 4-11. Effects of Tracer History: Room Temperature Digestion of Nonadsorbable Pa^{233} Tracer in 7N HNO_3.

techniques will be more adaptable than solvent extraction, owing to the high specific activity of protactinium and the susceptibility of solvents to radiation damage (see Sect. 4.4.3).

4.4.3 Changes in Silica Gel and DIBC Resulting from Irradiation
(G. I. Cathers, S. S. Brandt)

Three samples of silica gel were irradiated in a Co^{60} source in contact, respectively, with air, water, and 1 M nitric acid for an exposure of 6.8×10^8 r, equivalent to an energy dose of 2400 watt-hr per liter or to 5 hr of operation of a silica gel sponge with a Pa^{233} concentration of 10 g/liter. There was no detectable change in color or physical appearance in any sample. A water absorption test showed that the adsorption capacity of the two wet-irradiated samples had increased slightly (1.5%) over that of nonirradiated material. This is probably within experimental error, although it may indicate that the character of the absorptive surface has been favorably modified by polar groups from radiation-induced reactions in the aqueous phase. Calculations were made on the basis that the power produced by protactinium in decaying to U^{233} is 48 watts per gram. Test dosages equivalent to several months of operation should be used to obtain definite evidence on the stability of silica gel to radiation. Some practical experience of the Isotopes Production Division has indicated that degradation of particle size by severe radiation could present difficulties with continuous operation of columns owing to such factors as increasing pressure-drops and partial plugging.

A sample of DIBC irradiated in a Co^{60} source for an exposure equivalent to 190 watt-hr per liter showed no discoloration or development of acidity. Evaporation indicated that 3.2% nonvolatiles had formed in contrast to the absence of nonvolatiles in nonirradiated material. The G value for formation of nonvolatiles was therefore about 2.7, which is in line with other reported work on stability of organic materials to radiation.*

---

* G. I. Cathers, "Radiation Effects in Chemical Processing," ORNL CF-53-9-196 (Sept. 24, 1953).

Serious decomposition of DIBC may therefore be expected. A concentration of 10 g of Pa^{233} per liter would lead to about 8% conversion to nonvolatile material in 1 hr. Perhaps an equal amount would be converted to low boilers or noncondensable gases. Use of DIBC in an ordinary solvent extraction-stripping cycle with small contact time and low Pa^{233} concentration would lead to proportionately less decomposition. However, nothing has yet been established about the effect of radiation products, e.g., long-chain polymers, in extraction and stripping behavior. There is some evidence in the literature to indicate that organic solvents can be protected from radiation by addition of a stabilizer. This should be investigated not only in reference to DIBC, but to other solvents as well.

APPENDIX

5.1 Preliminary Investigation of a TBP Extraction Process for Recovering U^{233} from the CU Stream*

(B. G. Ryle)

Preliminary studies have been made to aid in the designing of a tributyl phosphate (TBP) extraction process as a possible alternate to the present ion exchange method for purifying and concentrating the U^{233} product stream (CU) from the Thorex process.

In general, the alternate process involves increasing the uranium concentration by evaporation; this step is followed by a preferential TBP extraction and aqueous stripping of the U^{233} from the Th^{232}, and the resulting aqueous uranyl nitrate solution is concentrated by evaporation. The effect of the initial boildown of the CU stream upon the extent of TBP decomposition and the concentration of the acid and heavy metal components appear as primary considerations. A tentative flowsheet outlining a TBP extraction system will be considered if the boildown process gives a product stream to which this method of separation can be applied. The relative merits of an acid versus an acid-deficient system are to be determined.

The results obtained from batch boildowns of nonradioactive synthetic CU solutions (see Table 5-1) indicate that the TBP decomposition products in the final concentrate are not present in sufficient amounts to cause large uranium losses in the subsequent TBP extraction process. The low rate of decomposition appears dependent on the condition that direct heating of the vapor phase during evaporation be avoided. The TBP present in solution in the CU stream undergoes rapid steam distillation, results indicating that approximately 85% is removed before a concentration ratio of 5 is reached (Fig. 5-1). The phosphate concentration in the residue is greater than in the original solution, but the total amount of phosphate present is less (see Table 5-2). This indicates that a portion of the initial phosphate is chemically combined in the residue with the heavy

---

* Summary of ORNL CF-53-5-20, "Preliminary Investigations of a TBP Extraction Process on Recovering U^{233} from the Thorex Process CU Stream," by B. G. Ryle.

Table 5-1

Components of Synthetic CU Stream

Component	Concentration in CU Stream	Form in Which Added
Uranium	0.1 mg/ml	$UO_2(NO_3)_2 \cdot 6H_2O$
Thorium	0.038 mg/ml	$Th(NO_3)_4 \cdot 4H_2O$
HNO_3	0.1 N	15.8 M HNO_3
TBP	0.25 mg/ml	Distilled
Fluoride ion	0.038 mg/ml	NaF
Iron	0.8 ppm	$Fe(NO_3)_3 \cdot 6H_2O$
Nickel	3.2 ppm	$Ni(NO_3)_2 \cdot 6H_2O$

Table 5-2

Change in Phosphate Concentration During Evaporation

Boildown Ratio	Phosphate Concentration (mg/ml)		Total Weight of Phosphate (mg)	
	Initial	Final	Initial	Final
91	0.31	0.733	620	66
100	0.001	0.042	4	1.68
42	0.024	0.038	48	2
100	0.031	0.047	62	1

[redacted]
Dwg No 18897-A

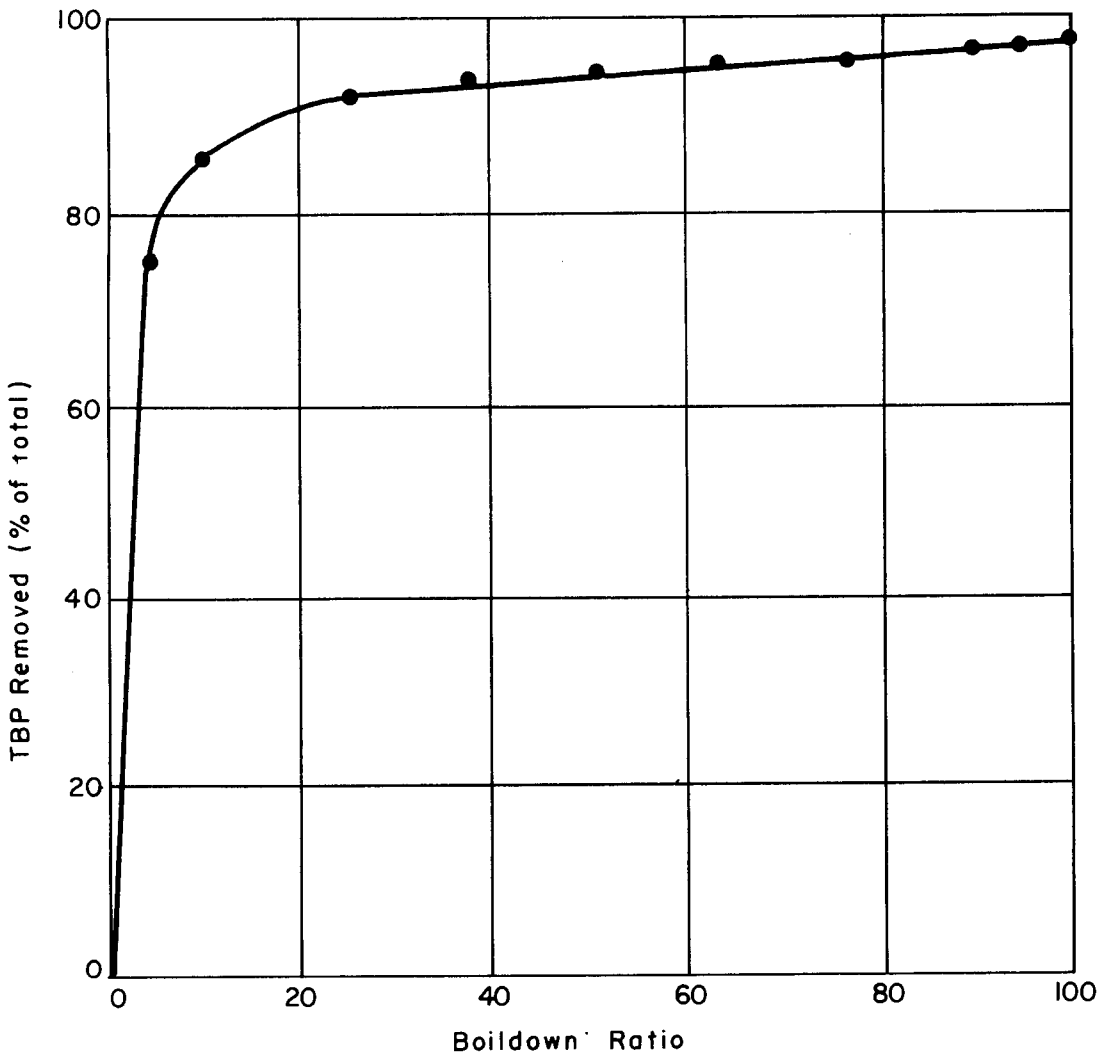

Fig. 5-1. Percentage Removed of the Total TBP Initially Present as a Function of the Boildown Ratio. Batch boildown. Initial volume 2 liters, initial nitric acid concentration 0.15 *M*.

metals present.

The uranium concentration increases in direct proportion to the increase in boildown ratio, indicating no loss during the evaporation process (Fig. 5-2). The increase of nitric acid concentration is also regular up to a boildown ratio of approximately 70, above which the rate of loss increases (Fig. 5-3).

The thorium concentration increases regularly up to a boildown ratio of approximately 30, at which point ThF_4 begins to precipitate. Further increases in concentration by evaporation cause increased precipitation. It has been found that an increase in the molar ratio of fluoride ion to thorium ion decreases the boildown ratio at which ThF_4 begins to precipitate. The thorium apparently exists in two forms in solution, e.g., as the free Th^{4+} ion and as molecular ThF_4. Increasing the concentration of the constituent ions by evaporation shifts the equilibrium in favor of the molecular species. Upon further concentration, the ThF_4 solubility is exceeded and it precipitates. A boildown ratio between 25 and 30 appears satisfactory for avoiding thorium precipitation. A modified pretreatment of the sample solution using aluminum nitrate prior to colorimetric determination of thorium is necessary where relatively high fluoride ion concentrations exist, as in the present work.

Preliminary batch countercurrent studies were made in order to ascertain the most efficient flow ratios, salt strength, and TBP concentrations to use. The results of the two runs made to date indicate that it may be necessary to change from the acid extraction system used at present to a modified acid-deficient aluminum nitrate system, using diban, in order to attain the salt strength necessary for better extraction, permitting lower extract acidity and less uranium loss (see Table 5-3).

[redacted] Dwg No 18894-A

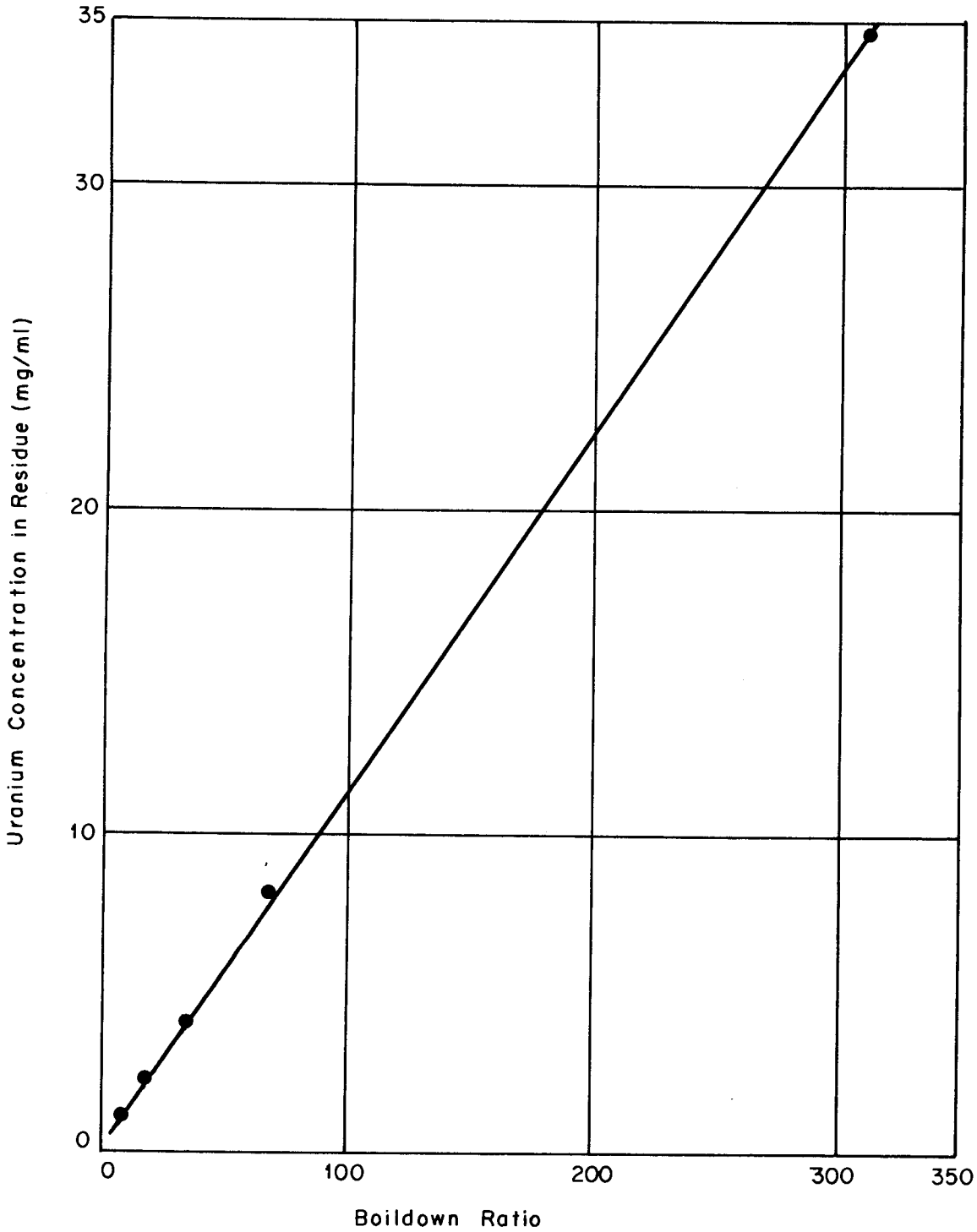

Fig. 5-2, Uranium Concentration in Residue as a Function of the Boildown Ratio.
Initial uranium concentration = 0.112 mg/ml.

[redacted] Dwg No 18898-A [redacted]

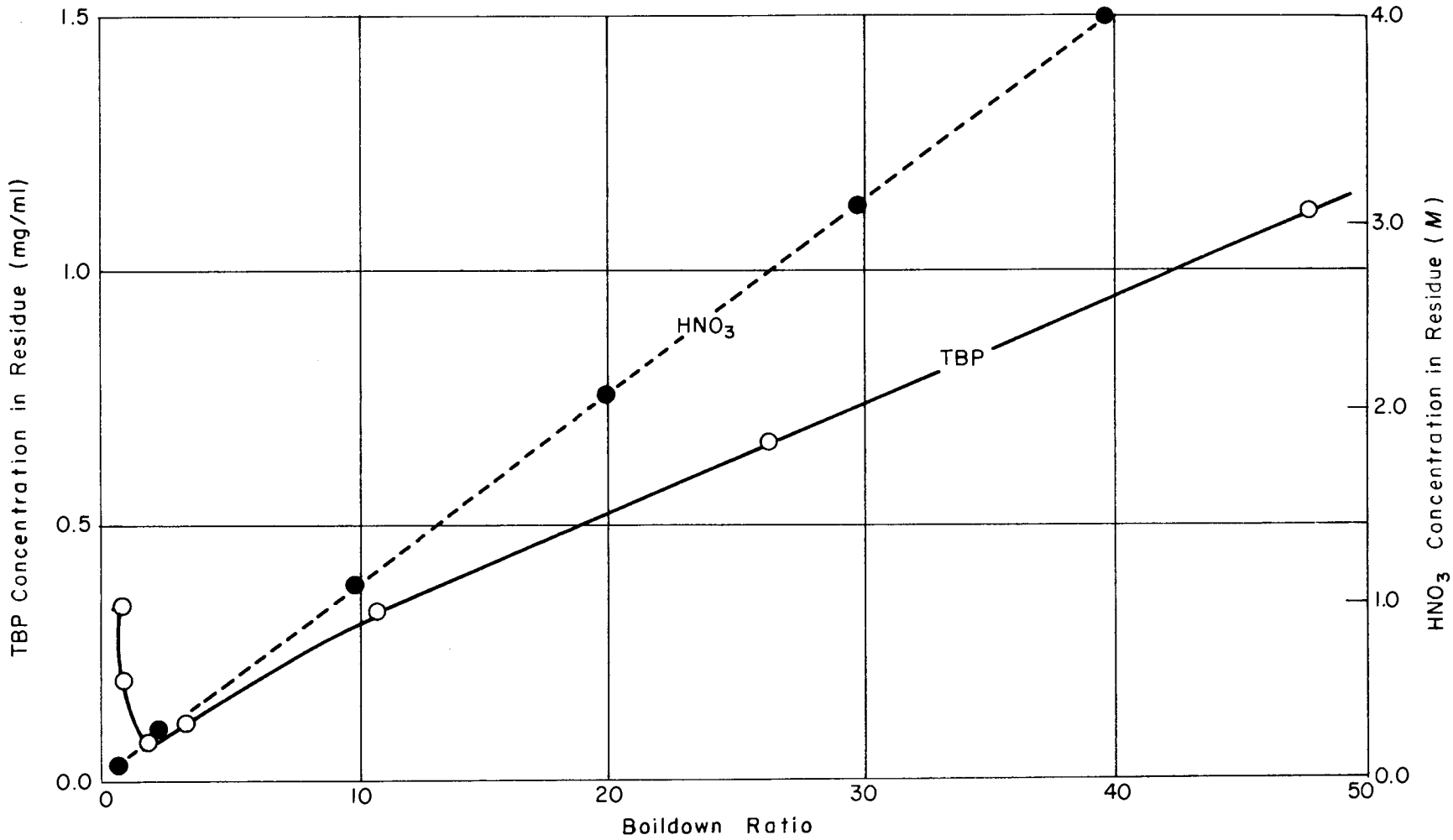

Fig. 5-3. Nitric Acid and TBP Concentrations in Residue as a Function of the Boildown Ratio. Batch procedure. Initial volume 2 liters, initial TBP concentration 0.345 mg/ml, initial nitric acid concentration 0.10 *M*.

Table 5-3

Data from Batch Countercurrent Extraction of Uranium

Run 1

Feed: 0.021 M $UO_2(NO_3)_2$, 0.008 M $Th(NO_3)_4$, 3.65 N HNO_3; 5.14 mg of U and 0.180 mg of Th per milliliter
Scrub: 2.80 N HNO_3
Organic: 9% TBP, 91% Amsco 125-90W
Feed/scrub/organic flow ratio: 10/1/2
Data taken after 3 vol changes; initial stage added after 1.5 vol changes; initial feed, 50/1 boildown, filtered to remove ThF_4 ppt.

Run 2

0.014 M $UO_2(NO_3)_2$, 0.0007 M $Th(NO_3)_4$, 2.54 N HNO_3; 3.23 mg of U and 0.159 mg of Th per milliliter
0.95 N HNO_3
10% TBP, 90% Amsco 125-90W
10/1/2
Data taken after 3 vol changes; initial feed, 30/1 boildown, not filtered

Stage	Organic Phase			Aqueous Phase			D.C.'s (O/A)		
	Uranium (mg/ml)	Thorium (mg/ml)	HNO_3 (N)	Uranium (mg/ml)	Thorium (mg/ml)	HNO_3 (N)	U	Th	HNO_3
Run 1									
6Sc	18.5	0.09	0.13	4.0	0.01	2.90	4.62	9.0	0.045
4Sc	20.5	0.08	0.11	5.0	0.02	2.98	4.10	4.6	0.039
2Sc	22.0	0.10	0.12	5.5	0.02	3.00	4.00	5.0	0.040
1E	22.0	0.12	0.13	5.0	0.03	3.50	4.50	4.1	0.037
3E	20.0	0.09	0.14	4.0	0.02	3.50	5.00	4.5	0.040
5E	8.5	0.04	0.20	1.0	0.07	3.50	8.50	0.6	0.057
Run 2									
6Sc	7.60	0.037	0.075	3.80	0.022	0.984	2.00	1.70	0.076
4Sc	11.63	0.061	0.095	6.73	0.045	0.990	1.73	1.35	0.096
2Sc	12.13	0.090	0.100	7.95	0.056	1.05	1.53	1.61	0.095
1E	13.20	0.090	0.190	3.37	0.290	2.35	3.91	0.31	0.081
3E	11.88	0.094	0.190	2.95	0.241	2.35	4.03	0.39	0.081
5E	9.00	0.044	0.185	1.95	0.199	2.35	4.61	0.22	0.079
7E	3.20	0.020	0.185	0.67	0.187	2.30	4.76	0.11	0.080

5.2 Solvent Diluent Studies
(J. E. Savolainen)

5.2.1 Philosophy of Solvent Handling in the Thorex Process

The diluent pretreatment and the solvent recycle treatment are designed to remove from the system those deleterious constituents which have a high probability of interaction with fission products or emulsifying agents, thus causing a distribution of radioactivity. Elimination of erratic behavior is essential if provision for protection of the operators from the radiation present in the materials processed is to be made with an assuring safety factor. Erratic behavior of the radioactivity, leading to a varying contamination of the product, would dictate subsequent recycle or reprocessing operations of a nonroutine nature. The carrying out of nonroutine operations on a large scale is both expensive and hazardous.

An increased complexity is imposed at each step in the processing of highly radioactive materials when biological shielding for the protection of operating personnel is required. Therefore it is advantageous to eliminate or reduce the frequency of even a simple radioactive operation by carrying out a nonradioactive operation. The proposed pretreatment of the diluent is a nonradioactive operation of this type.

Diluent Pretreatment. Untreated hydrocarbon diluents (e.g., Amsco 125-90W) contain small and varying amounts of unstable constituents which react with the aqueous process solutions to produce substances that cause formation of stable emulsions and interfacial solids. The pretreatment of the diluent is designed to reduce the amount of these deleterious materials before the diluent enters the process. Such removal is simpler and less expensive at this stage than later, when shielding would be required because of the radioactivity present. Reduction in the amount of these impurities in the diluent will increase the time that the system can operate before the solids and emulsions interfere, thus permitting more flexible scheduling and therefore more economic operation.

Solvent Recovery. With extended recycling of the solvent, decomposi-

tion products of TBP, e.g., MBP and DBP, are formed as well as diluent decomposition products. These decomposition products reduce the efficiency of the separation process by decreasing the effectiveness of the partition of thorium from the uranium. They are the most probable cause of solvent contamination.

Two methods have been proposed for the removal of these chemical contaminants of the solvent; one is by treating the solvent with a sodium carbonate solution followed by centrifugation, the other by treating the solvent with an aqueous slurry of calcium hydroxide followed by centrifugation.

The advantages and disadvantages in the immediate application of the two recycle solvent treatment methods are:

Advantages	Disadvantages
Sodium Carbonate Method	
1. Equipment is available and in use and would not increase the design load	1. The solvent is not effectively decontaminated and might cause excessive exposure of operating personnel
2. Technics of operation have been worked out and are understood by the operators	2. The waste volumes and solids are greater than with the calcium hydroxide method
Calcium Hydroxide Method	
1. It produces a superior solvent for column operation	1. Optimum contactor operation is not known for plant-scale use
2. It is more effective in decontaminating the solvent	2. Operators do not have extensive experience with the new type of contactor required by this method

The Unit Operations data indicate that the calcium hydroxide-treated recycle solvent permits full-capacity operation of the extraction columns, and that the operating characteristics of the solvent treated in this manner are superior to those of the sodium carbonate-treated solvent. Apparently

the sodium carbonate-treated solvent can be used within the design limits of the process. However, the higher level of contamination which occurs with the sodium carbonate-treated solvent is expected to increase the contamination of the product and to increase the difficulty of handling the solvent between the solvent recycle treatment and the point of entry into the extraction column. If the contamination of the product reaches a level requiring a second cycle reprocessing, the waste volumes will be increased and the overall efficiency of the process will be reduced.

Solvent Disposal. After the solvent has been in operation for an extended length of time, the presence of some of the diluent decomposition products which cannot be removed by the solvent recycle treatment may make it necessary to dispose of the solvent. A large portion of the solvent may be recovered by a vacuum distillation method. Butanol, water, and low-boiling decomposition products could be removed first from the solvent by distillation at about 35°C and 50 mm Hg. The diluent can then be distilled at about 50°C and 1 mm Hg. The TBP can then be recovered at 110°C and 1 mm Hg. The recovered diluent would contain only the most stable constituents and would be the ideal diluent for solvent makeup.

5.2.2 Nitric Acid Degradation of Diluents Catalyzed by Mercury

The behavior of diluents is being studied to determine a method for evaluating diluent stability. First to be studied was the effect which mercury ions have on the rate of color and solid impurity formation when Amsco 125-82 is contacted with 10 M HNO_3. The observations (see Table 5-4) indicate that (1) mercury catalyzes the degradation of the diluent, (2) an interfacial solid is an intermediate degradation product, and (3) on further degradation, the solid becomes aqueous- and organic-soluble.

The experiments were carried out by contacting 30-ml portions of Amsco 125-82 with 25 ml of 10 M HNO_3. The mercury concentration in the aqueous phase was varied from 0 to 0.1 M in six different samples. The phases were agitated mechanically in tubes for 100 hr in such a way that they were inverted

Table 5-4

Results of Contacting Amsco 125-82 with 10 M HNO_3 Containing Increasing Amounts of Mercury

Observation after 100 hr contacting at room temperature

Hg Conc. in Aqueous Phase (M)	Comments
0	A thin film of pale yellow interfacial solid appeared between the two phases; both phases were practically colorless
0.0005	A thin layer of brown amorphous solid covered the interface; both phases were practically colorless
0.001	A moderately thick layer of brown solid accumulated at the interface and was dispersed over the expanded interface on agitation; as the phases separated after agitation, the solid formed increasingly thick membranes at the phase boundary and interfered with phase disengagement; both phases were light yellow
0.005	The amount of solid was judged to be about five times the amount in the sample contacted with the 0.001 M Hg^{++} solution; the behavior of the brown solid was similar; the color density of the phases was judged to be about twice that of the previous sample
0.01	The amount of solid was judged to be half that in the sample containing 0.005 M Hg^{++}; the behavior was similar to that of the sample containing 0.001 M Hg^{++}; the color of the phases was several times more intense than in the previous samples
0.1	No interfacial solid appeared in this sample; the interfaces were bright and both phases were clear; the phases were intensely colored compared to those in the previous sample

and reinverted eight times in 10 sec. Comparisons of the amount of color in the aqueous and organic phases as well as the amount of interfacial solids were made.

The increase and then the decrease in the amount of interfacial solid with increasing mercuric ion concentration as well as the progressively increasing intensity of the color in the two phases may be explained as follows:

1. The mercury catalyzes the degradation of the diluent, and the amount may govern the degree of degradation which takes place.

2. As the degradation proceeds, solid-forming materials are produced. These appear to be insoluble in both the aqueous and the organic phases; they also appear to be surface active.

3. As the degradation reactions are increased by a greater concentration of mercury, the interfacial solids react further, forming aqueous- and organic-soluble species which appear to be highly colored.

Because the intermediate degradation reaction products are removed from the organic phase in the form of an interfacial solid, the reactions may be difficult to follow by chemical analyses of the organic phase. Diluents that produce large amounts of degradation products as observed by the intensity of the color in the liquid phases may form intermediate products that form interfacial solids.

The low mutual solubilities of hydrocarbons and aqueous nitric acid solutions reduce the rate of reaction. In this case most of the primary reactions are expected to occur at the liquid interface. After the diluent molecule has reacted by oxidation or nitration, its solubility in the aqueous phase is increased. This in turn increases the probability of further reaction.

Diluents are expected to be degraded faster in the presence of TBP because of the increased solubility of the nitric acid in the organic phase.

5.3 Spectrographic Analysis of Organic Solid Contaminants (J. E. Savolainen)

Concentrates of interfacial solids, obtained from 1200 liters of Purex solvent (30% TBP in untreated Amsco 123-15) and Thorex solvent (41% TBP in untreated Amsco 125-90W) during Unit Operations tests of the calcium hydroxide solvent recovery system (see ORNL-1518, p. 40), have been separated into four distinct species. Qualitative spectrographic analyses indicated the presence of several elements in the following rough order of prevalence: Al, Si, Ca, Th, P, Pd, Mn, Fe, Cr, Ni, Mg, Cu, Ti, V, Mo, B, Zr, Zn, Sn, Pb. One of the species, which was extremely black in color and relatively insoluble in inorganic acids, carried most of the radioactivity associated with the solids as well as the bulk of the above elements. The order of impurities in this solid material was: Al, Ca, Si, Pd, Mn, Fe, Cr, Ni, Mg, Ti, Mo, Cu, Sn, Zr, V, Th, B, and Pb. It was the only one of the four species found to contain V, Mo, Sn, and Pb and to show an absence of P. The nature of the organic radicals associated with these elements is unknown at present.

5.4 Tentative Chemical Flowsheet for the Decontamination and Recovery of U^{235} from Irradiated Uranium-Aluminum Alloys, Using a 1.5% TBP Extraction* (E. L. Nicholson)

In accordance with discussions with Dr. E. P. Wigner relative to a cost evaluation of various alternate processes for separation of U^{235} from irradiated U^{235}-aluminum alloys, several scouting runs in laboratory batch countercurrent equipment were carried out to survey the possibilities of developing a process patterned after the Interim-23 process.

The data indicate that a chemical flowsheet using (1) 1.5% TBP as the solvent, (2) aluminum nitrate as the salting and scrubbing agent, (3) silica gel adsorption for removal of trace colloidal gamma emitters, and (4) uranium isolation by ion exchange would provide a simple and direct process (one extraction cycle) for high recovery and decontamination of U^{235} (see

---

* Originally published as ORNL memorandum CF-53-7-183, "Tentative Chemical Flowsheet for the Decontamination and Recovery of U-235 from Irradiated Uranium-Aluminum Alloys Using a 1.5% TBP System," by E. L. Nicholson (July 24, 1953).

Fig. 5-4). Uranium losses of less than 0.01% and gross beta decontamination factors greater than 10^7 can be predicted throughout the overall extraction, adsorption, and ion-exchange cycles.

This process presupposes the HNO_3-Hg^{++} dissolution of the alloy for feed preparation and the attendant storage of radioactive aluminum nitrate wastes.

Experimental Work. Six countercurrent runs (see Table 5-5) were carried out to establish conditions for uranium extraction and decontamination. Zirconium was observed to be the limiting fission product contaminant through the extraction cycle, but this contamination was controllable by use of sulfate ion. Unusually high decontamination factors were experienced for rare earths, ruthenium, and niobium. The use of nitric acid—preconditioned Amsco 125-82 as the TBP diluent was credited with permitting low retention of activities, particularly those of a colloidal nature.

The uranium losses in the extraction step were about 0.015% and in the stripping step, about 0.001%. Beta decontamination factors in the extraction step were: gross, 8.0×10^5; TRE, $> 6 \times 10^6$; Ru, 8×10^4; Zr, about 10^5; and Nb, $> 3 \times 10^5$. Through the stripping stage the gross beta decontamination factor was increased to 1.3×10^6 and the ruthenium decontamination factor to about 1.3×10^5.

The addition of 0.02 M sulfuric acid to the aqueous feed and scrub solutions effected a 57-fold increase in the zirconium decontamination factor over that obtained in previous demonstration runs in which sulfate ion was not used. The final beta activity was only 30 c/m per milligram of uranium, i.e., about 30% of the natural uranium background. Beta activity retained in the waste organic stream was only 80 c/m/ml in this run, which is a tribute to nitric acid stabilization of diluents by preconditioning.

Discussion. Full-level-activity demonstrations are considered essential to proof of decontamination factors of higher orders than reported here. Significant statistical errors in counting at the low activity levels observed in this run contribute to a degree of uncertainty in measurements so near the natural background, and presently available equipment does not permit our

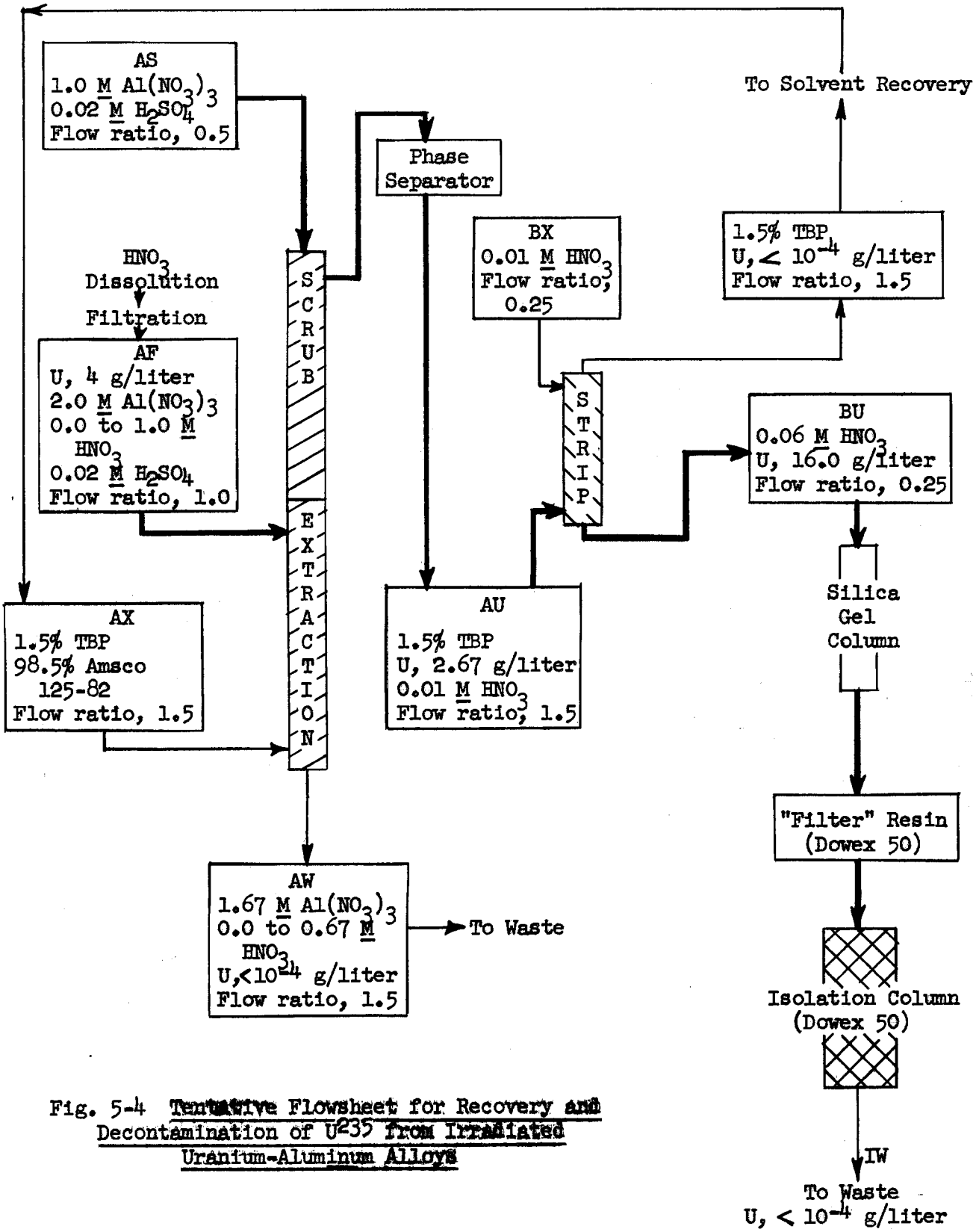

Fig. 5-4 Tentative Flowsheet for Recovery and Decontamination of U^{235} from Irradiated Uranium-Aluminum Alloys

Table 5-5

Summary of Conditions Observed in the A and B Columns of the 25 Process Flowsheet

Aqueous feed: 2.0 M $Al(NO_3)_3$, 4.0 g of uranium per liter, -0.2 to 1.0 M HNO_3, 0.02 M H_2SO_4, containing beta activities as follows: gross, 1.2×10^8; TRE, 8.27×10^7; Ru, 1.1×10^7; Zr, 4.7×10^6; and Nb, 5.5×10^6; digested about 1 hr at room temperature. (In E-1)
Aqueous scrub: 1.0 M $Al(NO_3)_3$, 0.02 M H_2SO_4. (In S-1)
Organic extractant: 1.5% TBP in HNO_3-preconditioned Amsco 125-82. (In E-4)
Aqueous strip: 0.01 M HNO_3. (In 3-St)
Flow ratios: F/S/O/St = 1/0.5/1.0/0.25
Number of stages: 4 extraction, 6 scrub, 3 strip

Stage	Solution Components	Organic	Aqueous	D.C.(O/A)	E.F.(O/A)
B3-St	HNO_3 (M)	<0.002	0.1	---	---
	U (g/liter)	0.00004	0.0074	0.005	0.03
	Gross β (c/m/ml)	80	125	0.64	3.8
B1-St	HNO_3 (M)	0.006	0.058	0.1	0.6
	U (g/liter)	0.084	15.8	0.0053	0.03
	Gross β (c/m/ml)	140	370	0.39	2.4
A6-S	Al (M)	---	1.0	---	---
	HNO_3 (M)	0.008	0.006	1.3	3.9
	U (g/liter)	2.72	1.31	2.05	6.2
	Gross β (c/m/ml)	100	100	1.0	3.0
	Ru β	~90	~90	~1.0	~3.0
A4-S	Al (M)	---	1.0	---	---
	HNO_3 (M)	0.013	0.016	0.8	2.4
	U (g/liter)	2.94	2.3	1.28	3.9
	Gross β (c/m/ml)	140	205	0.68	2.1
	Ru β	90	130	0.7	2.1
A2-S	Al (M)	---	1.0	---	---
	HNO_3 (M)	0.014	0.022	0.63	1.9
	U (g/liter)	3.18	2.96	1.1	3.3
	Gross β (c/m/ml)	300	985	0.3	0.9
	Zr β	54	577	0.094	0.28

Table 5-5 (Cont.)

Stage	Solution Components	Organic	Aqueous	D.C.(O/A)	E.F.(O/A)
A2-S (Cont.)	Tre β (c/m/ml)	~11	---	---	---
	Ru β (c/m/ml)	260	120	2.2	6.6
	Nb β (c/m/ml)	~12	160	---	---
A1-E	Al (M)	---	1.67	---	---
	HNO_3 (M)	0.032	0.77	0.04	0.04
	U (g/liter)	3.63	1.25	2.9	2.9
	Gross β (c/m/ml)	5.5×10^3	7.5×10^7	7.3×10^{-5}	7.3×10^{-5}
	Zr β (c/m/ml)	3.0×10^3	4.8×10^5	6.2×10^{-3}	6.2×10^{-3}
	TRE β (c/m/ml)	60	5.7×10^7	1×10^{-6}	1×10^{-6}
	Ru β (c/m/ml)	500	8.0×10^6	6.3×10^{-5}	6.3×10^{-5}
	Nb β (c/m/ml)	55	5.2×10^4	1×10^{-3}	1×10^{-3}
A3-E	Al (M)	---	1.67	---	---
	HNO_3 (M)	0.028	0.75	0.04	0.04
	U (g/liter)	0.08	0.006	13.3	13.3
	Gross β (c/m/ml)	2.5×10^4	7.7×10^7	3.2×10^{-4}	3.2×10^{-4}
	Zr β (c/m/ml)	1.56×10^4	4.2×10^5	3.7×10^{-2}	3.7×10^{-2}
	TRE β (c/m/ml)	1.1×10^4	5.8×10^7	1.9×10^{-4}	1.9×10^{-4}
	Ru β (c/m/ml)	250	7.6×10^6	3.3×10^{-5}	3.3×10^{-5}
	Nb β (c/m/ml)	250	5.0×10^4	5×10^{-3}	5×10^{-3}
A4-E	Al (M)	---	1.67	---	---
	HNO_3 (M)	---	0.7	---	---
	U (g/liter)	---	0.0007	---	---
	Gross β (c/m/ml)	---	7.3×10^7	---	---

demonstration of higher levels. However, it is felt that this extraction process combined with the silica gel column, the Dowex 50 resin filter and the Dowex 50 resin ion exchange uranium isolation column, as utilized in the Interim-23 program, would permit development of a very efficient and straightforward process for isolation and decontamination of U^{235}.

Provision of six stages in the extraction and six in the scrubbing section of the A-column would probably make it possible to set the AF aluminum nitrate concentration at 1.9 M ± 10%, and the uranium concentration could be 4.0 g/liter ± 10% without seriously affecting operations or efficiency. However, large changes in uranium concentration, for example, as a result of differences in the percentage of uranium in the alloy or percentage burnup, should be compensated for by process changes, particularly in the AX flow ratios; e.g., the AX flow ratio would be 0.75 for 2.0 g/liter but 2.25 for 6.0 g/liter. These factors result from the percentage uranium saturation and the capacity of the TBP present in the extractant.

The extreme uranium distribution coefficient in the stripping system, i.e., 0.005 (O/A) or 200 (A/O), indicates that organic/aqueous (AU/BX) flow ratios of 100 to 200 would permit recovery of U^{235} at high concentrations (1.0 to 2.0 M), if desirable, as a substitute for concentration by ion exchange. An additional beta decontamination factor of 40 to 80 would result from such a scheme owing to the higher beta distribution coefficient, i.e., 0.4 (O/A), permitting overall decontamination factors of the order of 5×10^7 through extraction and stripping. To take advantage of this scheme, however, development of semicontinuous contactor units would be required.

5.5 Decontamination of Thorium by Recrystallization Methods (W. T. McDuffee)

A tentative flow diagram for the refining and decontamination of mantle grade thorium nitrate is shown in Fig. 5-5. Rare earth contamination appears limiting and ruthenium is the contaminant most easily removed by this method. The results of a run in which the mantle grade thorium nitrate solution was spiked with Purex feed solution to obtain $\sim 10^6$ gross beta c/m/ml are shown in Table 5-6. The yield of the first crop of crystals was 40% (based on

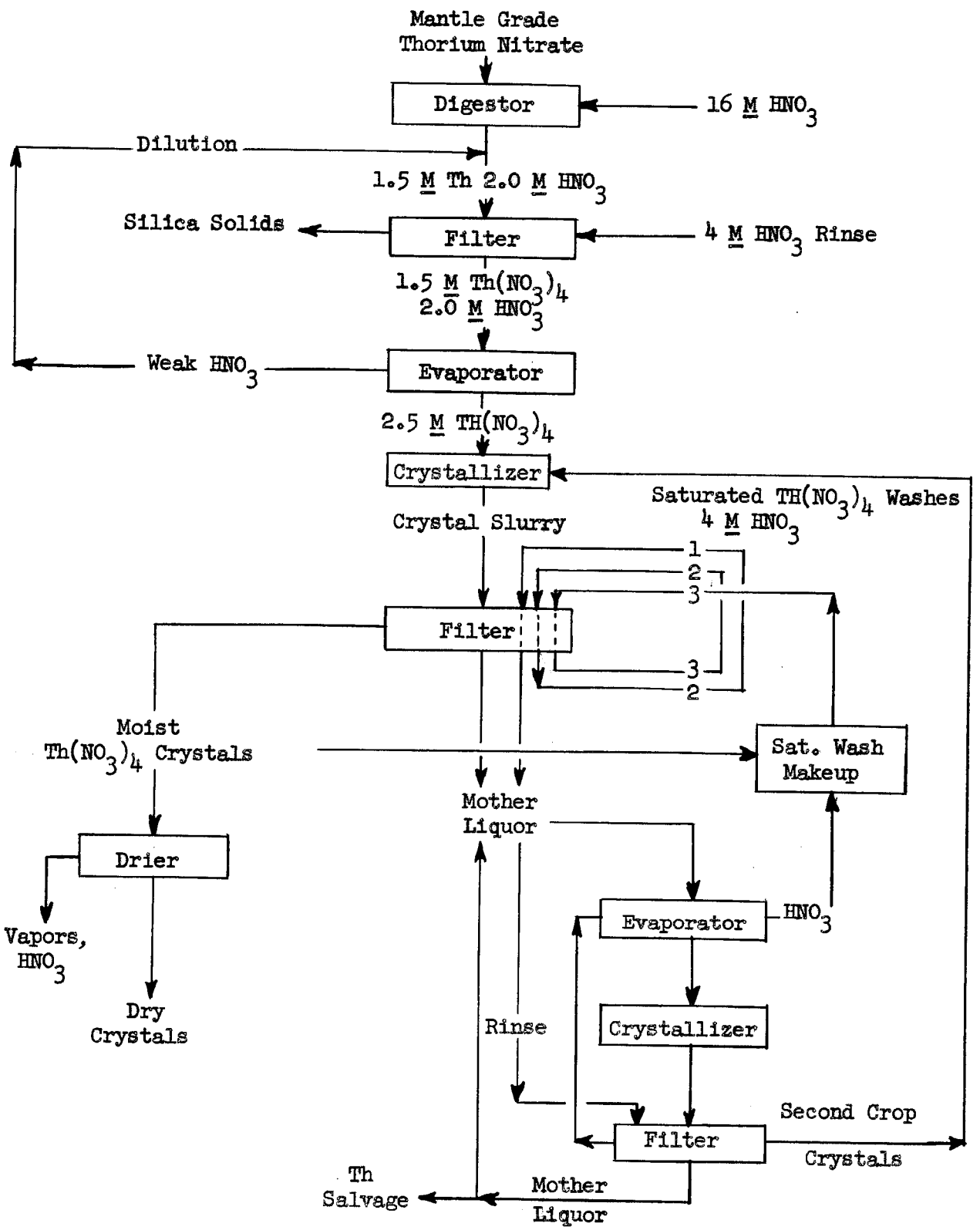

Fig. 5-5 Tentative Method for Purifying Mantle Grade $Th(NO_3)_4$ by Recrystallization.

thorium) and that of the second crop was 20%. The uranium separation factors from the thorium by the above method were, from the first and second crops of crystals, 4×10^4 and 2×10^4, respectively.

Tentative consideration has been given to possible uses of such procedures in the Thorex process.

5.6 Properties for Monitoring Sodium Carbonate Solution Concentrations and Consumptions

The results of pH and conductivity determinations made on aqueous sodium carbonate solutions show that the sodium carbonate concentration of the aqueous phase entering the solvent wash column cannot be determined by a pH reading, but that it can be with a conductivity reading if no other ionic materials are present (see Table 5-7 and Fig. 5-6). The reverse is true for the consumption of sodium carbonate in the aqueous phase within the column — it cannot be determined by a conductivity measurement, but it can be by a pH measurement (see Tables 5-8 and 9 and Figs. 5-7 and 8).

For the data on the relation between concentration and these physical properties, the properties of solutions of various concentrations were measured at about 25°C. The pH readings were made with a Beckman pH meter, model G, calibrated with a buffer solution of pH 10. The conductivities were determined with an Industrial Instruments, Inc. conductivity bridge, model RC, using a dipping conductivity cell which had a constant of 1.0.

For the data on carbonate consumption, two series of determinations were made of the change in conductivity and pH of sodium carbonate solutions as they were titrated with nitric acid. Conditions were set so that the properties would indicate the behavior which could occur in the aqueous solution of a sodium carbonate solvent wash column. The amount of water entering the aqueous phase from the solvent in expected to be negligible. Therefore, no dilution of the aqueous phase is expected to occur within the column.

Sodium carbonate solutions, 200 ml each of 0.1 M and 0.2 M, were titrated with 10.1 M nitric acid. The high nitric acid concentration was

Table 5-6

Decontamination of Mantle Grade Thorium Nitrate by Recrystallization

Mantle grade $Th(NO_3)_4 \cdot 4H_2O$ spiked 1 to 10^4 (based on final solution volume) with Purex feed solution, digested at 125 to 130°C for 4 hr with 16 M HNO_3 (8.3 g of hydrated salt to 1 ml of 16 M HNO_3), diluted to 1.5 M thorium concentration, and filtered to remove silica solids; concentrated and crystallized; crystals separated and cake washed with saturated refined thorium nitrate solution, 4 M in HNO_3.

Stream	Th (mg/ml)	Gross β (c/m/ml)	D.F.	Ru β (c/m/ml)	D.F.	Nb β (c/m/ml)	D.F.	TRE β (c/m/ml)	D.F.	Zr β (c/m/ml)	D.F.
Feed	337	1.30×10^6	---	5.89×10^4	---	2.14×10^4	---	7.85×10^5	---	1.48×10^5	---
Filtrate	362	1.27×10^6	---	6.03×10^4	---	1.57×10^4	---	7.85×10^5	---	1.15×10^5	---
Mother liquor	337	3.94×10^6	---	1.94×10^5	---	5.36×10^4	---	2.14×10^6	---	3.76×10^5	---
Wash No. 1	377.6	1.30×10^6	---	6.70×10^4	---	1.12×10^4	---	7.6×10^5	---	1.19×10^5	---
Wash No. 2	371.2	2.96×10^4	---	768	---	1.21×10^3	---	1.39×10^4	---	--	---
Wash No. 3	364	3.27×10^4	---	252	---	1.03×10^3	---	---	---	869	---
1st crop of crystals[a]	220	3.20×10^4	27	76	510	3.51×10^2	40	2.63×10^4	19	760	128
2nd crop of crystals[a]	205	1.41×10^5	6	475	76	3.34×10^3	40	1.23×10^5	4	5.05×10^3	18

(a) Dried crystals made up into ~1.0 M aqueous solution.

Table 5-7

The pH and Conductivities of Sodium Carbonate Solutions at 25°C

Sodium Carbonate Concentration (M)	pH	Conductivity ($ohms^{-1}cm^{-1}$)
0.04	10.60	0.0080
0.07	10.68	0.0131
0.10	10.68	0.0171
0.13	10.62	0.0216
0.16	10.62	0.0276
0.20	10.60	0.0298

Table 5-8

Conductivity and pH of 0.1 M Na_2CO_3 Titrated with HNO_3

200 ml of 0.1 M Na_2CO_3 titrated with 10.1 M HNO_3 at 25°C

Titer (ml of 10.1 M HNO_3)	pH	Conductivity ($ohms^{-1}cm^{-1}$)	Titer (ml of 10.1 M HNO_3)	pH	Conductivity ($ohms^{-1}cm^{-1}$)
0	10.85	0.0135	1.4	9.50	0.0142
0.1	10.70	0.0136	1.5	9.39	0.0142
0.2	10.55	0.0135	1.6	9.28	0.0143
0.3	10.40	0.0136	1.7	9.12	0.0143
0.4	10.30	0.0136	1.8	8.90	0.0144
0.5	10.20	0.0137	1.9	8.57	0.0145
0.6	10.12	0.0137	1.95	8.28	0.0145
0.7	10.15	0.0138	2.0	7.88	0.0149
0.8	9.98	0.0138	2.05	7.62	0.0146
0.9	9.90	0.0139	2.1	7.43	0.0147
1.0	9.83	0.0139	2.2	7.20	0.0147
1.1	9.75	0.0139	2.3	7.03	0.0149
1.2	9.67	0.0140	2.4	6.90	0.0150
1.3	9.58	0.0141	2.5[a]	6.80	0.0152

(a) A readily observable gas evolution occurred at this point.

Table 5-9

Conductivity and pH of 0.2 M Na_2CO_3 Titrated with HNO_3 [a]

200 ml of 0.2 M Na_2CO_3 titrated with 10.1 M HNO_3 at 25°C

Titer (ml of 10.1 M HNO_3)	pH	Conductivity ($ohms^{-1}cm^{-1}$)	Titer (ml of 10.1 M HNO_3)	pH	Conductivity ($ohms^{-1}cm^{-1}$)
0	10.83	0.0254	2.8	9.38	0.0278
0.2	10.56	0.0253	3.0	9.28	0.0282
0.4	10.40	0.0251	3.2	9.15	0.0286
0.6	10.30	0.0257	3.4	9.02	0.0284
0.8	10.20	0.0255	3.6	8.80	0.0286
1.0	10.10	0.0249	3.8	8.50	0.0292
1.2	10.00	0.0263	3.9	8.30	0.0286
1.4	9.90	0.0267	4.0	7.85	0.0294
1.6	9.85	0.0259	4.1	7.59	0.0292
1.8	9.75	0.0267	4.2	7.39	0.0294
2.0	9.70	0.0255	4.4	7.15	0.0296
2.2	9.60	0.0251	4.6	7.00	0.0301
2.4	9.50	0.0270	4.8	6.85	0.0303
2.6	9.46	0.0278	5.0	6.78	0.0303

(a) Gas evolution was observed during the entire titration.

[redacted]

[redacted]

Dwg No 22 530

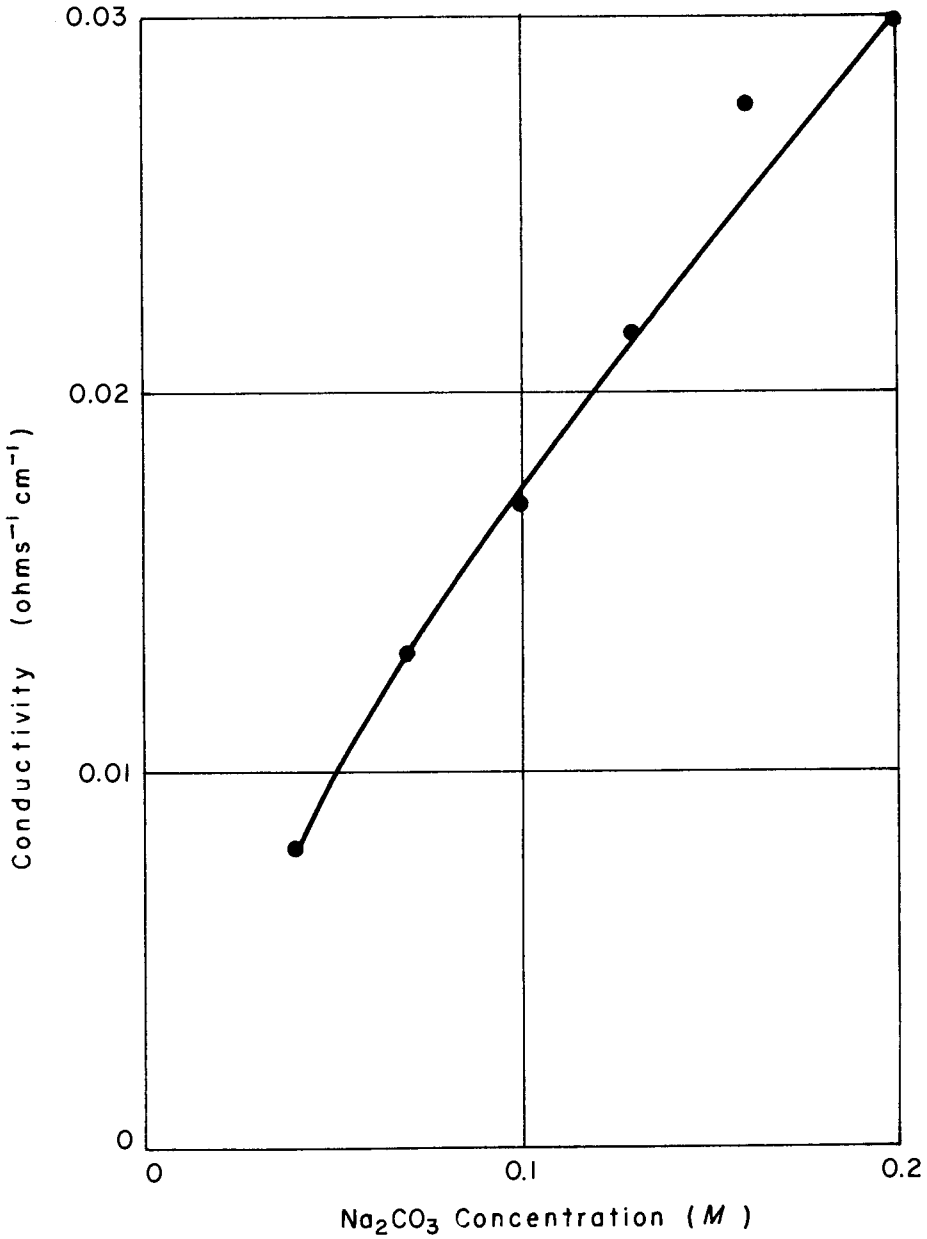

Fig. 5-6. Conductivity of Aqueous Na_2CO_3 Solution as a Function of Concentration at 25°C.

[redacted] [redacted]

Dwg No 22531

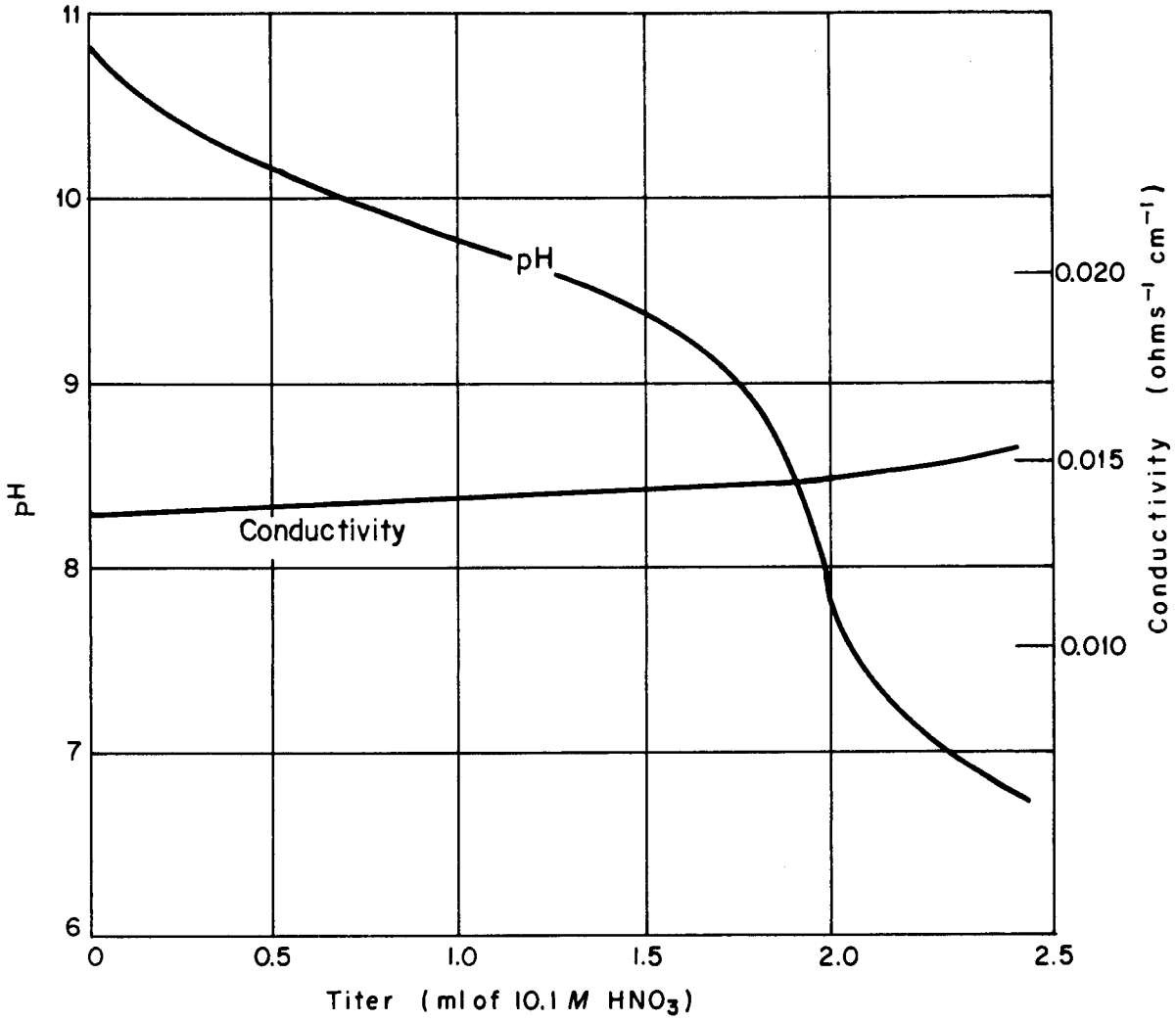

Fig. 5-7. Conductivity and pH of 0.1 *M* Na_2CO_3 Titrated with 10.1 *M* HNO_3.

[redacted]
Dwg No 22532

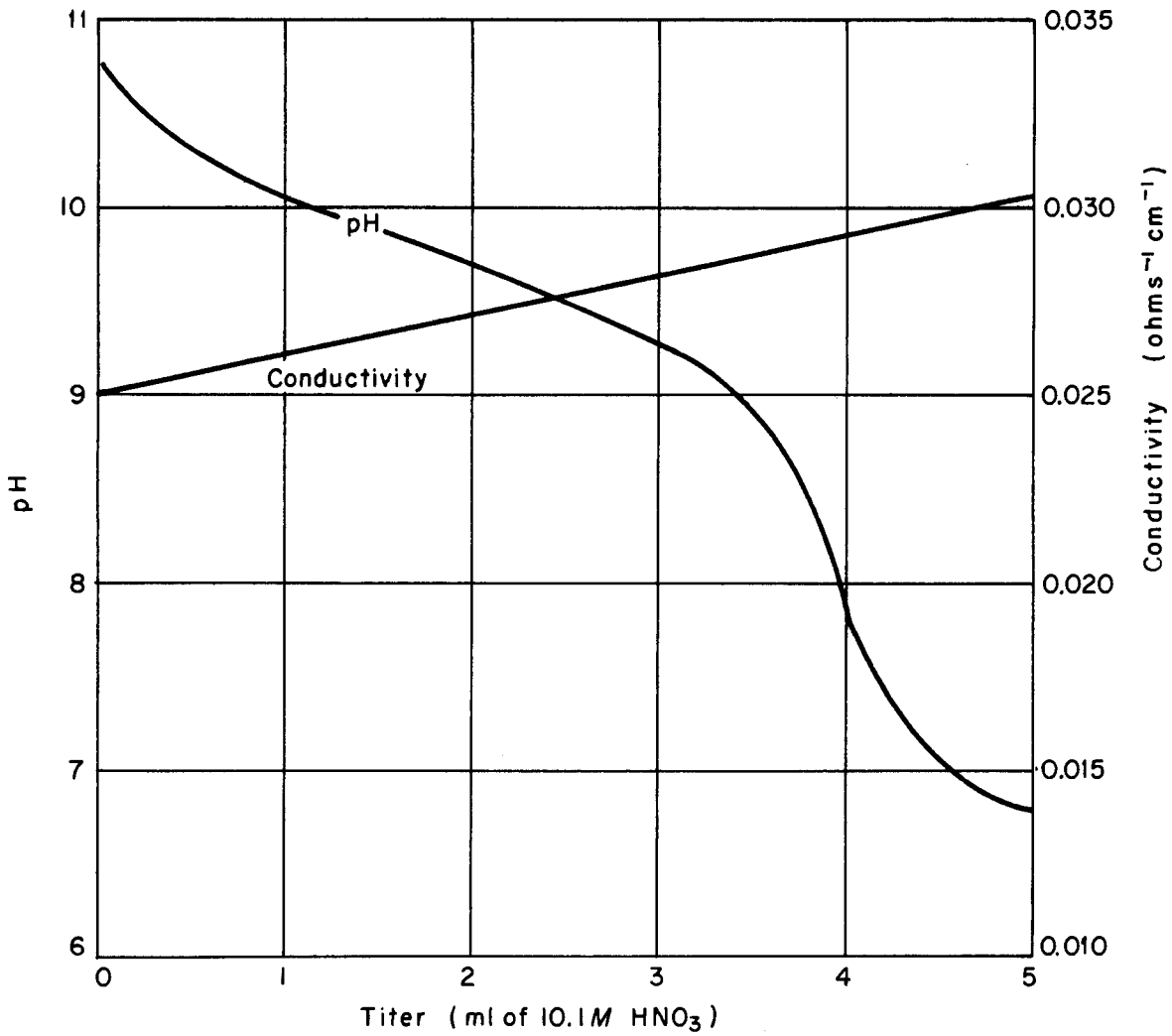

Fig. 5-8. Conductivity and pH of 0.2 *M* Na_2CO_3 Titrated with HNO_3.

used to reduce the diluting effect of the titrant on the carbonate solution. After each increment of acid was added, the pH and the conductivity were measured. The experiments were carried out at room temperature, about 25°C. The same instruments were used as mentioned above.

5.7 Composition of Diban Solutions (J. E. Savolainen)

Three samples of Diban solution supplied by vendor No. 1 and one sample of a solution supplied by vendor No. 2 were obtained for laboratory evaluation. The results of analyses of these samples and of a sample of Diban solution prepared at ORNL show (see Table 5-10) that ammonia may be produced during the dissolving of aluminum metal by aluminum nitrate solutions in the presence of mercury catalyst, which is the method used for preparing these solutions. Ammonia in the amounts found in these solutions is not expected to affect the Thorex process chemistry.

The total nitrogen determined by the Kjeldahl method exceeded the nitrogen value of the total anion concentration calculated as nitrate ion, and the difference between the two was greater than the ammonia nitrogen. This indicates that nitrogen may be present in the solution in some form other than nitrate or ammonia. The total anion concentration was determined by an ion exchange method which is used to determine anions other than OH^-. The ammonia was determined by distilling the sample in a caustic solution and titrating the distillate with acid.

Distillates from each sample were titrated in a sulfuric acid solution with potassium permanganate, but no significant amounts of reducing substances were found.

Spectrographic analyses (see Table 5-10) indicate that these samples are within the specifications given previously (ORNL-1518, p. 52).

5.8 Preparation of Soluble Niobium Nitrate Solutions for Tests of Protactinium Adsorbability on Silica Gel (M. R. Bennett)

A solution of soluble niobium nitrate, 0.02 M in Nb^{5+}, was prepared for use in tests of niobium inhibition of Pa^{233} adsorption. This was done by

Table 5-10

Results of Chemical Analyses of Diban Samples

Components	Vendor No. 1 Lot No. 13-RD-63	Vendor No. 1 Lot No. 13-RD-64	Vendor No. 1 Lot No. 13-RD-66	ORNL Sample	Vendor No. 2
Al^{3+} (M)	3.67	3.74	3.95	3.84	4.10
OH^- (M)	7.95	7.50	8.90	7.20	8.00
Total N by Kjeldahl (M)	6.00	5.80	5.29	4.68	5.27
NO_3^- by ion exchange	4.84	5.04	4.16	4.32	4.03
NH_3 by distillation (M)	0.51	0.55	0.73	0.09	0.0125
Total cations:					
3 x Al^{3+} (M) + NH_3 (M)	11.52	11.77	12.58	11.61	12.31
Total anions:					
OH^- (M) + NO_3^- (M)	12.79	12.54	13.06	11.52	12.03
OH/Al ratio	2.16	2.01	2.25	1.88	1.95
NH_3/OH ratio	0.064	0.073	0.082	0.013	0.0016
Spectrographic analysis					
Al	Very strong	Very strong	Very strong		Very strong
Fe, Si	Trace	Trace	Faint trace		Trace
Ca, Cu, Mg	Faint trace	Faint trace	Faint trace		Faint trace
Cr	Faint trace	Faint trace	Faint trace		Sought, not found
Mn	Sought, not found	Sought, not found	Sought, not found		Faint trace
Ag, V	Faint trace	Faint trace	Sought, not found		Sought, not found
B	Faint trace	Sought, not found	Sought, not found		Sought, not found
As, Au, Ba, Be, Bi, Cd, Co, Li, Mo, Na, Ni, Pb, Sb, Sn, Ti, Zn	Sought, not found	Sought, not found	Sought, not found		Sought, not found

adding 18.6 mg of niobium metal (200 mesh) to 19.0 ml of 2.0 M nitric acid containing 1.0 ml of 48% HF. This was heated to about 100°C; the time required for dissolution was 1 to 2 min. The niobium concentration could be increased by increasing the hydrofluoric acid concentration. However, it was desired to maintain the fluoride concentration of the stock solution at sufficiently low levels to permit, on dilution in AP test samples, fluoride concentrations no exceeding process conditions, i.e., 0.04 M.

5.9 Thorium Distribution at Equilibrium between the Aqueous and Organic Phases in the A-Column (J. E. Savolainen)

Data on the equilibrium distribution of thorium between the aqueous and the organic phases are needed to calculate the stage heights of the contacting column. The distribution for the A-column was determined at 24.5°C.

Two sets of data were determined for the extraction section (see Tables 5-11 and 12); in one the aqueous phase was 0.66 M in aluminum and 0.17 M acid deficient; in the other the aqueous phase was 0.57 M in aluminum and 0.153 M acid deficient. The difference in the salting effect is reflected in the divergence of the data at low thorium concentrations. At high thorium concentrations the data tend to be closer together because the salting effect of the thorium nitrate in the aqueous phase on its extraction tends to overcome the differences of the aluminum concentrations and its accompanying nitrate ions.

Data for the scrub section are shown in Table 5-13. The organic phase was the same as that used in obtaining the data for the extraction section. The aqueous phase was 0.6 M in aluminum and 0.6 M acid deficient.

Table 5-11

Thorium Distribution between Aqueous and Organic Phases in the A-Column Extraction Section

Organic phase: 50 ml of 41% TBP in pretreated Amsco 125-90W
Aqueous phase: 50 ml of 0.66 M aluminum, 0.17 M acid deficient
Equilibrated at 24.5°C

Aqueous Phase		Organic Phase	
Vol. (ml)	Th (mg/ml)	Vol. (ml)	Th (mg/ml)
47.0	122.0	53.0[a]	104.4
48.0	102.6	52.0[a]	97.8
47.8	80.0	52.2	91.4
47.9	60.0	52.1	79.0
47.8	48.0	52.2	76.4
48.0	38.0	52.0	69.6
48.5	28.5	51.5	61.0
48.9	19.0	51.1	50.0
48.8	13.5	51.2	41.0
48.5	7.70	51.5	27.1
49.5	3.70	50.5	13.4
49.5	1.80	50.5	6.58
49.5	1.08	50.5	3.63
49.7	0.173	50.3	0.682
49.7	0.085	50.3	0.349
49.7	0.018	50.3	0.062

(a) Two organic phases formed at high thorium concentrations; the average thorium concentration is calculated from the measured values of the two organic phases.

Table 5-12

Thorium Distribution between Aqueous and Organic Phases in the A-Column Extraction Section

Organic phase: 50 ml of 41% TBP in pretreated Amsco 125-90W
Aqueous phase: 50 ml of 0.57 M aluminum, 0.153 M acid deficient
Equilibrated at 25.5°C

Thorium Conc. (mg/ml)			
Aqueous Phase	Organic Phase	Aqueous Phase	Organic Phase
31.0	57.0	5.9	16.5
28.0	50.7	3.1	8.5
19.6	43.7	1.7	4.1
16.3	38.1	0.33	0.80
11.9	31.7	0.16	0.38
9.2	24.6	0.04	0.08

Table 5-13

Distribution of Thorium between Aqueous and Organic Phases in the A-Column Scrub Section

Organic phase: 41% TBP in pretreated Amsco 125-90W
Aqueous phase: 0.6 M aluminum, 0.6 M acid deficient
Equilibrated at 24.5°C

Thorium Conc. (mg/ml)			
Aqueous Phase	Organic Phase	Aqueous Phase	Organic Phase
133.4	88.8	49.5	43.0
114.0	81.3	43.0	35.0
91.0	78.8	32.0	22.0
86.5	73.6	24.3	11.0
76.3	67.2	14.8	4.5
68.6	59.0		